Cyclopentane hydrates – A candidate for desalination?

Son Ho-Van, Baptiste Bouillot, Jérome Douzet, Saheb Maghsoodloo Babakhani, Jean-Michel Herri

Cyclopentane hydrates – a candidate for desalination?

S.Ho-Van[1, 2]*, B.Bouillot[1]*, J.Douzet[1], S. Maghsoodloo Babakhani[1], J.M.Herri[1]

[1]*SPIN Center, Ecole des Mines de Saint-Etienne, SPIN, CNRS 5307, LGF, F-42023, Saint-Etienne, France;*

[2]*Oil Refinery and Petrochemistry Department, Hanoi University of Mining and Geology, Duc Thang, Bac Tu Liem, Hanoi, Viet Nam*

*Corresponding authors: son.ho-van@emse.fr (S.Ho-Van) and bouillot@emse.fr (B.Bouillot).

Abstract

This article presents a systematic review on the past developments of Hydrate-Based Desalination process using Cyclopentane as hydrate guest. This is the first review that covers all required fundamental data, such as multiphase equilibria data, kinetics, morphology, or physical properties of cyclopentane hydrates, in order to develop an effective and sustainable desalination process. Furthermore, this state-of-the-art describes research and commercialization perspectives. When compared to traditional applications, cyclopentane hydrate-based desalination process could be a promising solution. Indeed, it operates under normal atmospheric pressure, lower operation energies are required, etc… However, there are some challenges yet to overcome. A decision aid in the form of a diagram is proposed for a new cyclopentane hydrates-based desalination process. Hopefully, concepts reviewed in this study will suggest new ideas to advance technical solutions in order to make commercial hydrate-based desalination processes a reality.

Keywords: Review, Desalination, Clathrate Hydrates, Cyclopentane Hydrates, Seawater treatment.

1. Introduction

Seemingly abundant, clean water is a crucial resource for life on our planet. However, due to the increasing population, industrialization, global warming, agriculture activities, the shortage of clean water has become an urgent issue in many countries, especially in the Middle East and Africa [1,2]. Today, more than 1 billion people are denied the right to access clean water and about 2.6 billion people lack access to adequate sanitation [3,4]. Dirty water is the world's second biggest children killer [3]. For instance, in the Kingdom of Saudi Arabia (KSA), 60% of water demand is provided by desalination, that is to say about 10 Mm^3/day [5]. Expectations of KSA desalination demand in 2050 should be 60 Mm^3/day. Therefore, while mature technologies exist, processes for clean water production need to be optimized in regard to the enormous future

demand. Because of the practical unlimited supply capacity of sea-water, desalination has become an ever increasingly used method to produce fresh water [6]. A history of desalination research literature is detailed in Figure 1. As illustrated in figure, there has been a significant rise in research on desalination over the past decades. The most common studied methods have been: Thermal distillation, Reverse osmosis, Freezing, and Electro dialysis [7–10].

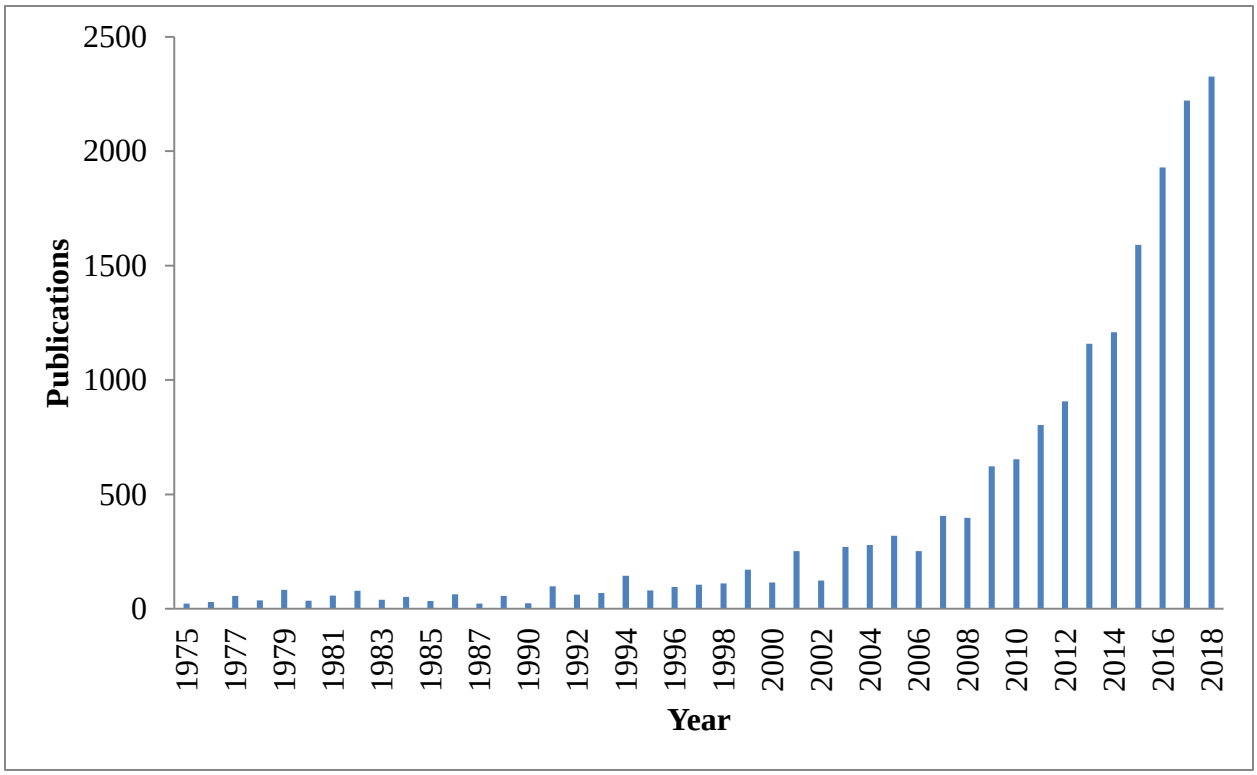

Figure 1. Frequency of desalination study in literature. Data from Web of Science with the keyword "desalination" (09/04/2019).

Recently, Clathrate hydrate–based desalination technique has attracted considerable interest [11–13]. Clathrate hydrates, or gas hydrates, are ice-like non-stoichiometric crystalline solid compounds that contain water molecules forming cages through a hydrogen-bonding system enclosing guest molecules, formed under high pressure and low temperature conditions [14]. This is usually the case for gaseous guest molecules (CO_2, CO, N_2, CH_4…). Other heavier guest molecules can form clathrate hydrates under atmospheric pressure (Cyclopentane (CP), Tetrahydrofuran…). Depending on size and nature of the guest molecules, water molecules can form different kind of cages that combine to form a crystal lattice according to three well-known

structures: I, II, and H. Since water is usually present in the oil and gas flowlines, gas hydrates are well known to plug pipelines [14]. Besides, several potential applications of clathrate hydrates have been investigated, such as gas storage [15–18], carbon dioxide capture [19,20], gas transportation [15,21], gas separation [22,23], air-conditioning [24–26], and of course seawater desalination [11,13,27,28].

Here is how water desalination works with Clathrates. During hydrate formation, water and guest molecules are incorporated into a new solid phase. It can be separated and recovered. Moreover, salts are excluded from the crystal phase. Therefore water and guest molecules can be retrieved after dissociation. If the guest is gaseous at standard conditions, only saturated gas remains inside liquid water. Consequently, clean "desalinated" water is obtained. If the guest molecule is not under vapor phase after dissociation, clean water is obtain providing that it can be separated after dissociation. Usual guest molecules studied for desalination applications are: CH_4, CO_2, C_3H_8, HCFC R141B, and CP.

As a matter of fact, gas hydrates-based desalination has been investigated for decades [10,12,29–38]. Despite that, hydrate-based technology is not used nowadays in desalination plants. There are several explanations: mostly energy consumption issues and technology immaturity [35]. However, a great deal of research has been done recently, and could provide a base for future hydrate-based desalination technology. In some studies, CP is suggested as an adequate guest candidate [39–45]. Indeed, CP forms clathrate hydrates with pure water under atmospheric pressure at 7°C. Especially, it is not miscible into water (solubility of 0.156 g/L at 25°C [46]). Therefore, it can be easily recovered from water after dissociation, and recycled for the desalination/cleaning process.

Note that CP act as a hydrate promoter for other applications, such as carbon capture, as described in detail by Herri et al. [22], or Zheng et al. [47]. It is a co-guest used to milder hydrate formation conditions when combined to other molecules such as N_2 [40,48–50], C_3H_8 [51], CO_2 [48,49,52–54], CH_4 [40,49,55,56], or H_2S [56]. Thus, the use of cyclopentane hydrates (CPH) for a combined gas capture and desalination process could be applicable and probably more interesting energetically.

Finally, this article provides a comprehensive, but non exhaustive, state-of-the-art review on CPH. It objective is to inform the scientific and industrial community the latest advances, and establishing the challenges to address when developing CPH-based desalination.

2. Phase equilibria of CPH

Phase equilibrium data of CPH in pure water and in presence of electrolytes are crucial for salt removal using CPH. Thermodynamic equilibrium data of CPH has been classified into three categories: CP+water, CP+water+electrolytes, and CP+water+other guests.

2.1. Phase equilibrium of CPH in pure water with and without surfactants

At ambient pressure, CP can form hydrate with pure water from 6.3°C to 7.7°C according to literature. The melting point varies in the literature, and can be lowered by adding surfactant such as SPAN 80. Table 1 presents literature results.

Table 1. Equilibrium temperature of CPH in pure water at atmospheric pressure with and without surfactant

Authors	Published year	Value (°C)	Method	Citation
Palmer et al.	1950	7.7	Quick dissociation	[57]
Davidson et al.	1973	7.7	Quick dissociation	[58]
Fan et al.	1999	7.07	"Pressure search" procedure	[59]
Dendy Sloan et al.	2008	7.7	Quick dissociation	[14]
Nakajima et al.	2008	6.6, 6.8, 7.1	DSC	[60]
Whitman et al.	2008	7.0	DSC	[61]
Nicholas et al.	2009	7.7	Quick dissociation	[62]
Zhang et al.	2009	7.02	DSC	[63]

Sakemoto et al.	2010	7.0[a]	Slow dissociation	[64]
Dirdal et al.	2012	7.7	Quick dissociation	[65]
Sefidroodi et al.	2012	7.7	Quick dissociation	[66]
Ambekar et al.	2012	6.3 (0.1% vol Span 80)$^{+}$	DSC	[67]
Zylyftari et al.	2013	7.11[a]	DSC	[68]
Zylyftari et al.	2013	6.57[b] (Span 80)$^{+}$	DSC	[68]
Han et al.	2014	7.8	Quick dissociation	[69]
Xu et al.	2014	7.7	Quick dissociation	[70]
Mitarai et al.	2015	7.1[a]	Slow dissociation	[71]
Martinez de Baños et al.	2015	7.2	*	[72]
Baek et al.	2015	6.7-7.2 (Span 20, 40, 60, 80)$^{+}$	DSC	[73]
Brown et al.	2016	7.7	*	[74]
Peixinho et al.	2017	6.7 (no Span 80)$^{+}$	Quick dissociation	[75]
		5.7 (0.0001 % mass Span 80)$^{+}$	Quick dissociation	[75]
		5.5 (0.001 % mass Span 80)$^{+}$	Quick dissociation	[75]
		7.7 (0.1 % mass Span 80)$^{+}$	Quick dissociation	[75]
Hobeika et al.	2017	7.0	*	[76]

Delroisse et al.	2017	7.2[c]	Slow dissociation	[77]
Ho-Van et al.	2018	7.7[a] 7.1[a]	Quick dissociation Slow dissociation	[28]
Delroisse et al	2018	7.05[d]	Stirred calorimetric cell	[78]

[+] in the presence of surfactant, * not acknowledge, DSC: Differential Scanning Calorimetry, Uncertainty range: [a] ±0.1°C, [b]±0.01°C, [c]±0.2, [d]±0.5°C.

Table 1 shows that there are actually two ranges of equilibrium temperatures in pure water: 7.7-7.8°C and 6.6-7.2°C. This can be explained by different experimental procedures used by the authors.

Equilibrium temperatures reported at 7.7-7.8°C range were obtain by quick dissociation method [28,65,66,69,79]. Unfortunately, the quick method tends to miss the correct dissociation temperature, because of the high dissociation rate. Therefore, the value of equilibrium temperature is usually overestimated.

One seemingly more reliable method is Differential Scanning Calorimetry (DSC) [60,61,63,68,73]. Equilibrium temperatures measured by DSC show a temperature range from 6.6°C to 7.2°C.

In addition, Sakemoto et al. [64], Mitarai et al [71], Ho-Van et al. [28], and Delroisse et al. [77] performed slow dissociation method and reported crystallization temperature of CPH of 7.0°C, 7.1°C and 7.2°C, respectively. The small variations could be attributed to heating rate differences. Sakemoto et al. [64], Mitarai et al [71], and Ho-Van et al. [28] used an increment of 0.1°C/hour, and 0.2°C/hour for Delroisse et al. [77]. Hence, equilibrium temperature reported by Delroisse et al. [77] is slightly higher. In another work, Delroisse et *al.* [78] reported the dissociation temperatures of 7.05°C (280.2 °K) by using a stirred calorimetric cell. Their method utilized an agitator to mix the fluid (CP+H_2O) in a calorimetric cell instead of static condition, as in a normal DSC method. This development is believed to provide more accurate data [78].

Martinez de Baños *et al.* [72] determined the equilibrium of 7.2°C which is very close to the values according to slow dissociation method [28,64,77], and DSC method [60,61,63,68,73]. Finally, the temperature range 6.6-7.2°C seems to be the most reliable and should be considered.
Besides, Ambekar et al. [67], Zylyftari et al. [68], Baek et al. [73], and Peixinho et al. [75] indicated that the use of a surfactant, such as Span, can reduce CPH equilibrium temperature. Indeed, hydrate crystallization is usually observed at the water – CP interface, while surfactant can modify the interfacial tension force. Hydrate formation is therefore affected by the surfactant [68,80]. Karanjkar *et al.* [81] stated that a mushy and porous structure, showing small needle-like crystals, is formed in presence of Span compared to polycrystalline shell structure in the absence of any surfactant. This porous structure hydrate may cause a reduction in dissociation point, referred to as the Gibbs–Thomson effect [68,82].
However, in the presence of 0.1% mass Span 80, corresponding to a concentration above Critical Micelle Concentration (CMC), the hydrate dissociation temperature is 7.7°C, according to Peixinho et al. [75]. At this concentration, surfactants cover the whole water droplet and the morphology of the hydrate is hence slightly denser. Consequently, dissociation would require a higher temperature [75].
In terms of pressure dependency, by applying a pressure-search method [83], Fan et al. [59] reported that CPH formation conditions are within the temperature range of 0.21-7.07°C for a pressure range of 6.9-19.8 kPa. The measured equilibrium data are detailed in Table 2. Fan et al. indicated that the quadruple point is 7.07°C at 19.8 kPa involving four phases: liquid water (L_w), liquid CP (L_{cp}), hydrate (H), and vapor CP (V_{cp}). This point is very close to the equilibrium temperature reported elsewhere [58,60,61,63,64,68,73] at atmospheric pressure, involving only three phases: L_w - H -L_{cp}.

In the desalination process, atmospheric pressure condition is more favorable than high pressure or even vacuum like conditions. However, the data reported by Fan et al. [59] are also very useful for salt removing from seawater under vacuum especially in association with membrane [84] or simply vacuum distillation [85].
Under higher pressures, Trueba et al. [86] reported hydrate (H) – aqueous liquid (L_w) – CP-rich liquid (L_a) phase equilibrium data. They indicated that the equilibrium temperature was nearly independent of pressure due to the low compressibility of the two fluids and the one solid phase.

This indicates that, without any gas molecule, CPH dissociation temperature is almost constant with pressure increase [86]. High pressure condition is out of the question in CPH pure based – desalination because of a significant increase in the energy required.

Table 2. Three phase (V-L_w-H) equilibrium data of CPH in pure water [59]

Phase	Temperature (±0.01°C)	Pressure (±0.1kPa)
L_w-H-V_{cp}	0.21	6.9
	1.19	8.1
	2.08	9.2
	3.34	11.2
	4.36	13.2
	5.72	16.3
	6.72	18.9
L_w- L_{cp}-H-V_{cp}	7.07	19.8*

* Upper quadruple point

Table 3. CPH phase equilibrium data at high pressure

Phase	**Temperature** (±0.02°C)	**Pressure (MPa)** (±3% of reading)
L_w-H-L_a	6.75	2.55
	6.79	5.05
	6.87	7.55
	6.85	10.03
	6.88	12.55

2.2. Phase equilibrium of CPH in the presence of salts

Obviously, to design an actual CPH based-desalination process, it is essential to have sufficient phase equilibrium data of CPH in the presence of diverse salts [28]. However, only few published datasets are available.

Zylyftari et al. [68] reported a set of equilibrium data in the presence of NaCl at a wide range of concentration, from 0 up to 23% mass by using DSC method. This method was also used by Baek et al. [73] for CPH equilibrium at 3.5% mass NaCl concentration.

Kishimoto et al. [87] used slow stepwise dissociation method to determine the dissociation points with an increment of 0.1°C/h at NaCl concentration from 5 to 26.4% mass fraction. Likewise, Sakemoto at al. [64] provided results in the presence of 3.5% NaCl and synthetic seawater. Delroisse et al. [77] reported 5 dissociation temperatures with NaCl present (0, 1, 2, 3, 4% mass NaCl) by using the slow dissociation method with an increment of 0.2°C/hour. Moreover, Ho-Van et al. [28,88] reported numerous equilibrium data for CPH in the presence of NaCl, KCl, NaCl-KCl, $CaCl_2$, Na_2SO_4, $MgCl_2$, $MgCl_2$-NaCl, or $MgCl_2$-NaCl-KCl under a wide-range of salt concentrations.

CPH equilibrium data in the presence of salts in the open literature are presented in Table 4, and Figure 2.

There are slight variations concerning dissociation temperature at 3.5% NaCl between four studies of Han et al. [69], Sakemoto et al. [64], Baek et al. [73], and Ho-Van et al. [28]. Han et al. [69] used the quick dissociation procedure leading to a higher value (6.6°C) compared to others. Among the three other data, Baek et al. [73] reported the lowest dissociation temperature of 4.57°C, while Ho-Van et al. [28] and Sakemoto et al. [64] recorded 5.0°C and 5.5°C, respectively. This is due to the presence of SPAN surfactant, used by Baek et al. [73]. It decreased the equilibrium temperature due to Gibbs–Thomson effect [82], as stated by Zylyftari et al. [68].

In addition, at 3.4% NaCl, Zylyftari et al. [68] reported that the equilibrium temperature of CPH is 5.28°C. This value is slightly higher than the value of 5.0°C at 3.5% NaCl provided by Ho-Van et al. [28].

Table 4. Literatures on equilibrium temperature of CPH in the presence of salts

Salts	Salt concentration range (% mass)	Method	Published year	Citation
NaCl	3.5	Slow dissociation[a]	2010	[64]
Synthetic seawater	*	Slow dissociation[a]	2010	[64]
NaCl	5-26.4	Slow dissociation[a]	2012	[87]
NaCl	0 – 23	DSC[a]	2013	[68]
NaCl	3.5	Quick dissociation	2014	[69]
NaCl	3.5	DSC	2016	[73]
NaCl	0 – 4	Slow dissociation[b]	2017	[77]
NaCl	0 – 23	Slow dissociation[a]	2018	[28]
KCl	0 – 20	Slow dissociation[a]	2018	[28]
NaCl-KCl	0 – 22	Slow dissociation[a]	2018	[28]
$CaCl_2$	0 – 25	Slow dissociation[a]	2018	[28]
Na_2SO_4	0 – 6	Slow dissociation[a]	2018	[88]
$MgCl_2$	0 – 20	Slow dissociation[a]	2018	[88]
$MgCl_2$-NaCl	0 – 22	Slow dissociation[a]	2018	[88]
$MgCl_2$-NaCl-KCl	0 – 22	Slow dissociation[a]	2018	[88]

* 2.6518% NaCl, 0.2447% $MgCl_2$, 0.3305% $MgSO_4$, 0.1141% $CaCl_2$, 0.0725% KCl, 0.0202% $NaHCO_3$, and 0.0083% NaBr. Uncertainty range: [a] ±0.1°C, [b] ±0.2°C.

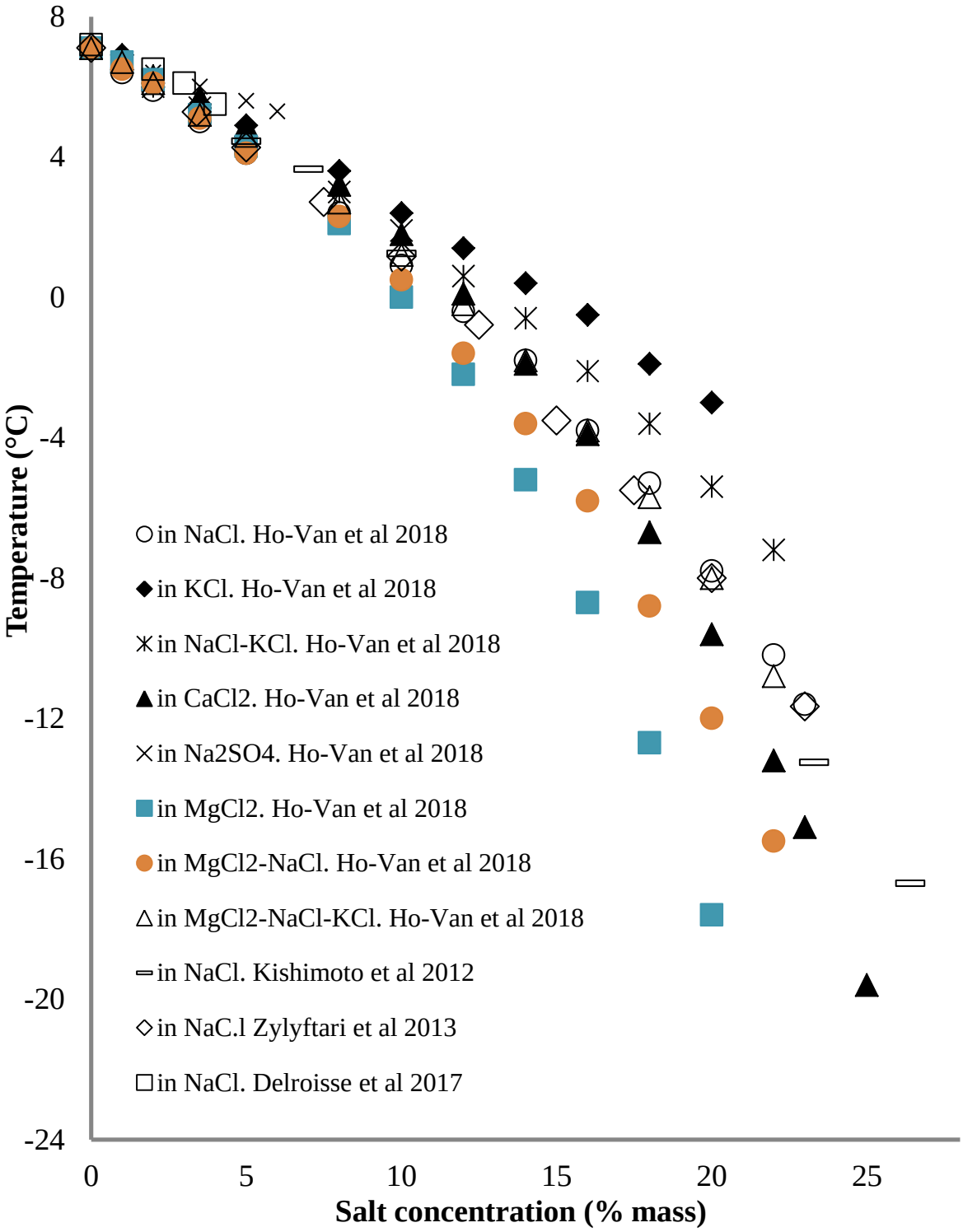

Figure 2. Equilibrium temperatures of CPH in the presence of salts from literatures [28,64,68,77,87,88]

The previous comparison indicates that the slow dissociation and DSC methods furnish more trustworthy data. Nonetheless, Delroisse et al. [77] offers a 2% NaCl dissociation temperature at 6.5°C ± 0.2°C. This is higher than the value of 5.9°C ±0.1°C reported by Ho-Van et al. [28]. This might be attributed to the higher dissociation rate (0.2°C/hour) used by Delroisse et al. [77] compared to Ho-Van et al. [28] (0.1°C/hour).

Figure 2 also points out that the hydrate formation temperature decreases quickly with increasing salt concentration, indicating that salt noticeably inhibits CPH thermodynamic equilibrium. Two well-known phenomena, "ion clustering" and "salting-out", are believed to reduce the hydrate formation temperatures, as clearly explained elsewhere [14,28,89].

Note bene: salt concentration increases during hydrate formation due to the consumption of pure water. When the salt concentration reaches saturation, precipitated salt can appear. Hence, solid salts can be recovered at the bottom of the bulk, while CPH lay above the aqueous phase. For instance, it happens easily for some salts such as Na_2SO_4 at 6% mass fraction [88], or $PbCl_2$, $CaSO_4$, and Ag_2SO_4 whose solubilities are very low into water. Therefore, their crystallization can occur quickly after CPH formation.

2.3. Phase equilibria of mixed hydrates containing CP as a co-guest

Clathrate hydrates can form in the presence of multiple guests beside CP. Therefore, some efforts used a secondary guest alongside CP for desalination process (Cha et al. [90], and Zheng et al. [47]). Results show that these mixed clathrate hydrates can improve salt removal efficiency compared to pure CPH. One promising idea is to combine CP with another guest molecule, and by this mean to couple desalination to another hydrate-based application, such as gas capture, gas hydrate exploitation (CH_4 for instance), or gas separation. Hereby, energy involved in the integrated process could be optimized, and salt removal efficiency could increase [20,47,91].

Table 5 provides range of thermodynamic equilibrium data of the mixed hydrate containing CP as a co-guest.

Table 5. Equilibrium conditions of mixed hydrate containing CP as a co-guest

Note: pure water implies distilled or only under laboratory conditions

Hydrate formers	Aqueous solution	Temperature range (K)	Pressure range (Mpa)	Citation
Binary				
CP – CO_2	Simulated produced water: 8.95 % mass	280.15 – 289.15	3.1	[90]
CP – CO_2	NaCl: 3.0% mass	271.89 – 292.21	0.55 – 3.59	[47]
CP – CO_2	NaCl: 0, 3.5, 7.0, 10.0, 15, 25% mass	269.8 – 292.4	1.18 – 3.33	[92]
CP – CO_2	Pure water	280.16 – 291.57	0.08 – 4.88	[52]
CP – CO_2	Pure water	284.6 – 291.6	0.49 – 2.58	[53]
CP – CO_2	Pure water	275.5 – 285.2	0.42 – 0.59	[20]
CP – CO_2	Pure water	284.3 – 291.8	0.35 – 2.52	[93]
CP – CO_2	Pure water	281.55 – 290.25	0.15 – 1.92	[94]
CP – CO_2	Pure water	283.5– 287.5	0.761– 1.130	[95]
CP – CH_4	NaCl : 0, 3.5, 7.0, 10.0 % mass	284.4 – 301.3	0.480 – 16.344	[96]
CP – CH_4	NaCl : 0, 3.5, 7.0% mass	288.5 – 296.9	3.26 – 1.09	[39]
CP – CH_4	NaCl : 3.5% mass	283.15 – 298.15	0.48 – 10.15	[97]
CP – CH_4	(K^+ , Na^+ , Mg^{2+} , Ca^{2+})	292.68 – 295.06	2.50 – 2.51	[98]
	(Cl^- ,SO_4^{2-})	293.75 – 295.06	2.50 – 2.51	[98]
CP – CH_4	Pure water	282.8 – 300.5	0.157 – 5.426	[40]
CP – CH_4	Pure water	284.8 – 299.3	0.321 – 4.651	[56]
CP – CH_4	Pure water	287.5 – 303.0	0.62 – 8.61	[48]
CP – CH_4	Pure water	286.70 – 300.0	0.48 – 5.69	[41]
CP – N_2	Pure water	282.9 – 289.1	0.641 – 3.496	[40]
CP – N_2	Pure water	285.9 – 302.0	1.68 – 24.45	[50]
CP – N_2	Pure water	284.7– 296.0	1.27– 10.4	[48]

CP – O_2	Pure water	289.4 – 303.3	2.27 – 21.69	[50]
CP – O_2	Pure water	286.0 – 297.1	1.03 – 9.10	[99]
CP – Methylfluoride	Pure water	287.9 – 305.9	0.138 – 2.988	[100]
CP – Kr	Pure water	283.8 – 308.5	0.116 – 7.664	[101]
CP – CH_2F_2	Pure water	280.45 - 299.75	0.027 - 1.544	[102]
CP – H_2	Pure water	280.68 – 283.72	2.70 – 11.09	[63]
CP – H_2	Pure water	281.3 – 288.3	4.34 – 32.	[50]
CP – H_2	Pure water	280.83 – 284.01	2.50 – 12.50	[86]
CP – H_2	Pure water	280.70– 284.31	2.463 – 14.005	[103]
CP – H_2	Pure water	283.4	10	[104]
CP – H_2S	Pure water	295.4 – 310.0	0.150 – 1.047	[56]
CP – Light mineral oil	NaCl : 0 – 23% mass	257.8 0– 278.55	0.101325 (Atmospheric)	[68]
Ternary				
CP – N_2 – CH_4	Pure water	283.3 – 289.5	0.310 – 1.855	[40]
CP – N_2 – CH_4	Pure water	283.4 – 288.1	0.3 – 1.2	[105]
CP – CH_4 – Trimethylene sulfide	NaCl : 0, 3.5, 5, 7, 10% mass	289.01 – 303.77	1.11 – 12.49	[106]
CP – THF – CO_2	Pure water	285.2 – 293.2	0.42 – 2.92	[53]
CP – THF – CO_2	Pure water	274.0 – 289.6	0.29 – 0.97	[20]
CP – CO_2 – N_2	Pure water	286.73 – 293.04	2.00 – 6.51	[107]
CP – CO_2 – H_2	Pure water	284 – 291	1.5 – 7.23	[108]
CP – CO_2 – H_2	Pure water	270.15 – 276.15	2.88 – 4.90	[109]
CP – O_2 – N_2	Pure water	284.0 – 296.2	1.09 – 9.45	[99]
CP – O_2 – N_2	Pure water	281.25	2.49 – 3.95	[110]
CP – Light mineral oil – Halocarbon 27	NaCl : 0 – 23% mass	258.67 – 278.54	0.101325 (Atmospheric)	[68]

Quaternary				
CP – TBAB – CO_2 – N_2	Pure water	280.20 – 290.32	2.21 – 5.71	[107]
CP – nC_5H_{10} – Methylbutane – Methylpropane	Pure water	273.35 – 279.68	5.5×10^3 – 19.5×10^3	[59]
CP – CH_4 – N_2 – O_2	Pure water	288.0 – 293.1	0.89 – 2.60	[111]
Quinary				
CP – Cyclohexane – CH_4 – N_2 – O_2	Pure water	278.6 – 286.7	1.99 – 5.08	[111]

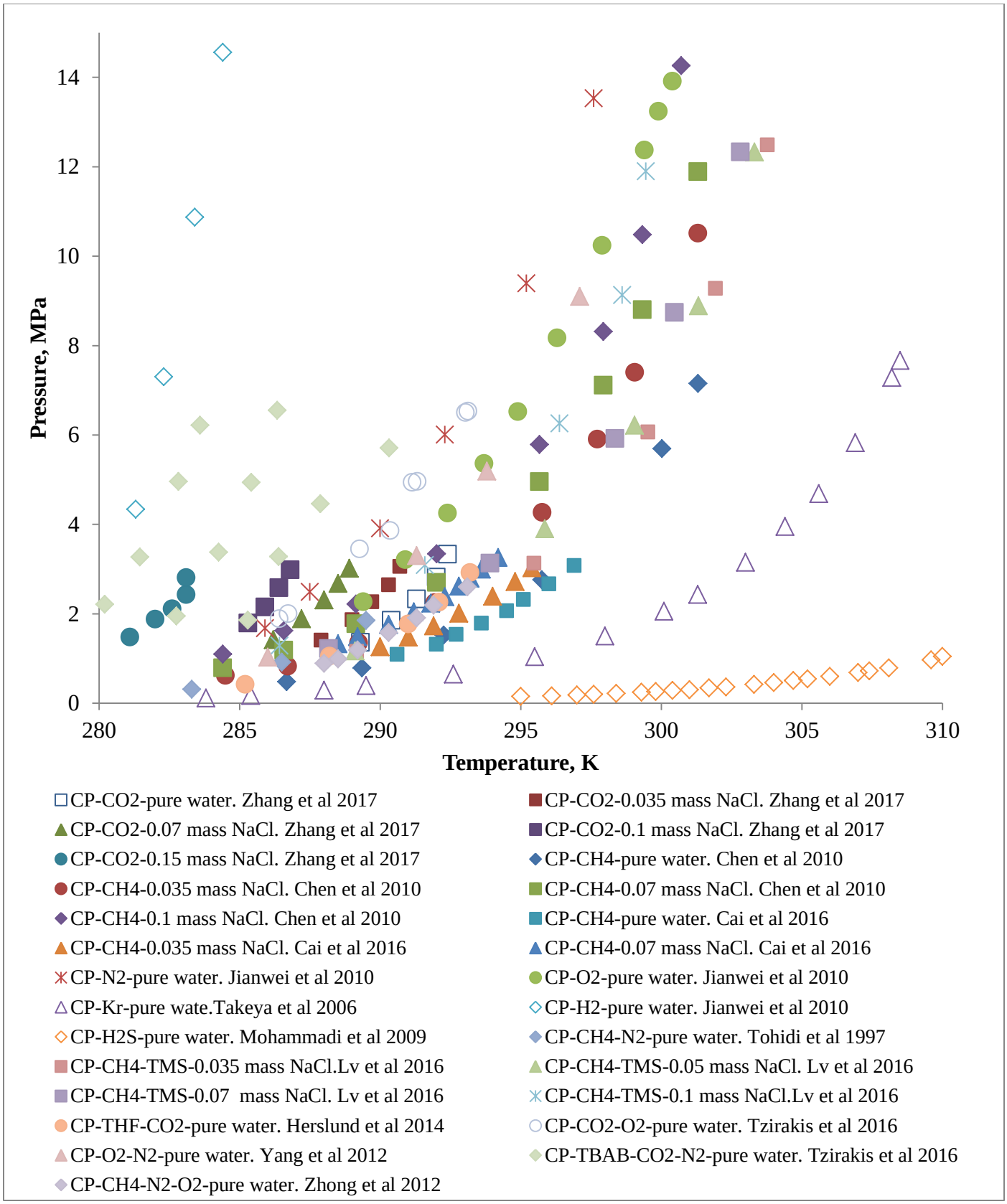

Figure 3. Equilibrium data of mixed gas hydrates containing CP in literature

Table 5 indicates that CO_2, CH_4, N_2, and H_2 are the four most common gases used to study mixed CPH. As seen from Figure 3, mixed CP-CH_4, CP-CH_4-O_2, CP-CH_4-N_2, CP-CH_4-TMS (Trimethylene sulfide) hydrates have been studied in pure water and in brine. Indeed, CH_4 is valuable fuel. Moreover, it is flammable and dangerously explosive at high pressure, especially when air, or just O_2, is present. As a result, CH_4 is not an auspicious hydrate former for CPH-based desalination, even though the hydrate formation conditions of the mixed CP-CH_4 hydrates are systematically milder than those of the mixed CP-CO_2, CP-O_2, CP-N_2, or CP-H_2 hydrates in fresh water and in brine.

Figure 3 also shows that CP-Kr and CP-H_2S can form mixed hydrates at the most favorable conditions [56,101] . However, Kr is a very expensive gas due to costly production process, from liquid air by a fractional distillation procedure. Plus, H_2S is a toxic, corrosive, and flammable gas. These gases cannot be considered as candidates for CPH-based desalination processes.

Figure 3 further indicates that the hydrate formation conditions of CP-O_2, CP-N_2, and CP-H_2 are all much harder to achieve than those of CP-CO_2 in pure water. As CO_2 is the most common and arguably famous greenhouse gas, the disposal of CO_2 has become a global concerns issue [17,19,112–115]. One of the ways to mitigate CO_2 emission is gas hydrate–based capture [116]. Furthermore, pressurized CO_2 streaming from CO_2 emission sources may be favorable for hydrate formation and the cost for pressurization can be decreased [117,118].

Note that CO_2 forms hydrate SI in pure water at 278.8 K at 2.33 Mpa according to the study of Zhang et al [92]. In the presence of CP, the binary mixture of CP-CO_2 can form SII hydrate at milder condition (291.3 K at 2.33 Mpa in pure water [92]) compared to the single CO_2 gas [90,92]. In this case, CP occupies large cages while CO_2 molecules occupy small cages. Hence, CP-CO_2 binary can be used for both desalination [44,47] and carbon capture [20]. Note that, in the case of flue gas, mixed CO_2-N_2-CP hydrates would be formed, and CO_2-H_2 for pre-combustion capture. Still, more studies are needed to improve gas hydrate based desalination and CO_2 capture processes in term of energy requirement, salt removal efficiency, and CO_2 storage capacity from a gas mixture in brine.

3. Kinetics of CPH formation

Kinetics is one key parameter for a process design. It is, in the present case, correlated to the rate of crystallization, water conversion efficiency, and therefore the number of separating steps, and

total operating cost. In this section, all published studies on kinetic of CPH formation are collected and investigated.

Table 6 lists the effects of several parameters on CPH formation kinetics in terms of nucleation and growth. In the next subsections, some details are provided to explain these phenomena.

Table 6. The effects of several considerations on kinetic of CPH formation

Considerations	Nucleation	Growth rate	Citation
Subcooling increase	↑	↑	[42,64,68,70–72,76,87,119–125]
Quantity of CP	↑	↑	[42,79,119,120,126,127]
Agitation speed increase	↑	↑	[39,60,70,119,124,125,128]
Use of ‘’Memory effect’’	↑	NA	[61,65,66,72]
Solid additives	↑	NA	[43,61,75,129,130]
Presence of salts	↓	↓	[39,45,68,72,77,87,119]
Presence of surfactants or polymers	↑	↑	[68,71,74,126,130–136]
Presence of surfactants or polymers	↓	↓	[65,74–77,121,131,137–140]
Presence of THF (0.01 - 0.05 % mass)	↑	↑	[139]
Presence of MeOH	↓	↓	[139]
Presence of activated carbon particles	↓	↓	[51]
Presence of free resins, biding resins, and residual Asphaltenes	NA	↓	[141]

where ↑: increase; ↓: decrease; NA: Not Acknowledge.

3.1 Subcooling and Agitation

The rates of hydrate nucleation [14,130,142–145] and growth [79,146–153] can be increased with the raise of the subcooling. Note that subcooling, ΔT_{sub}, is related to the driving force for the crystallization and defined as the difference between the system and the equilibrium temperature [87].

Xu et al. [70,124] indicated that the duration of CPH formation from salty water decreases with both the increase of subcooling and agitation speed. Martinez de Baños et al. [72] and Ho-Van et al [123] reported that the hydrate growth rate is observed to be proportional to subcooling. Indeed these conditions enhance mass and heat transfer between water/CP and the driving force for the hydrate formation.

Masoudi et al [79] stated that under mixing condition, the growth rate of CPH (1.9×10^{-5}–3.9×10^{-5} kg $m^{-2}s^{-}1$) is much higher than only flow condition (4.5×10^{-6} kg $m^{-2}s^{-}1$). Sakemoto et al. [64] and Kishimoto et al. [87] reported that the CPH nucleation location is at the CP-water interface because of the low solubility of CP in the aqueous phase. Consequently, agitation is needed to increase the kinetic of CPH formation.

Moreover, Cai et al. [125] observed that the rate of CP-CH_4 hydrate formation improves with the increase of the agitation rate. Indeed, this increase can lead to smaller CP droplets, as well as the splitting of hydrate shells covering CP droplets. Ergo, this enhances the CP-water contact area and then enhances the hydrate formation rate.

3.2 Addition of CP

Corak et al. [42] and Lim et al. [126] showed that the kinetic of CPH depends strongly not only on subcooling, but also on the quantity of CP. Faster growth was ascertained by increasing amount of CP. In fact, increasing the quantity of hydrate former improves mass transfer, diffusion and consequently escalates the number of nucleation locations for hydrate formation. However, for desalination, CP quantity needed to be minimized in accordance with other important parameters, in order to reduce the total cost.

3.3 “Memory effect’’

“Memory effect’’ corresponds to the empirical reduction of induction time by using a solution that has already formed crystals. This has been observed and used in laboratories to reduce drastically the induction time, especially for crystallization without agitation in small reactors. Some authors have investigated the influence of this phenomenon on hydrate formation [14,65,142,154–157]. Sefidrood et al.[66] concluded that the “memory effect” could enhance the nucleation of CPH formation. Using a small quantity of water from dissociated CPH at a temperature 2-3°C above the equilibrium, the CPH formation rate was observed to be much

faster than starting from fresh water. Consequently, in desalination, a small amount of the melted water from dissociation step can be recycled to the next CPH formation step in order to reduce the induction time. Of course, this is not a problem in case of a continuous process, or in presence of seeds.

3.4 Solid kinetic additives

Some kind of solids such as ice, silica gel, silica sand, rust, chalk, or clay have been studied to reduce hydrate nucleation time [37,65,158–161]. Zylyftari et al. [129] reported CPH formation at the ice – CP – brine phase contact line, which is believed to improve kinetics of hydrate crystallization [129]. Karanjkar et al [130] observed that, in this case, there is no induction time and nucleation takes place instantaneously as ice dissociates into free water. This fresh free water is then converted totally into CPH. Moreover, Li et al [43] indicated that addition of graphite promotes CPH formation. The graphite particles are composed of many flat carbon sheets (graphenes) that can provide heterogeneous sites for both ice and hydrate nucleation [43]. Other studies using nanoparticules can also be found, but not in presence of CP [162–164]. Nanofluids enhance crystallization kinetics as well [165].

3.5 Influence of salts

It is known that inorganic mineral salts affects significantly not only thermodynamics of CPH but also the kinetics of hydrate formation [39,146]. In the presence of salts, the equilibrium temperature is further shifted lower [14,28,64,68,72,77,88,89]. This leads to less subcooling, reducing hydrate growth and preventing the final water-to-hydrate conversion.

Kishimoto et al. [87] described that the nucleation and the growth rates of CPH are slowed down with increasing salt concentrations at a given subcooling. Moreover, Cai et al [39] reported that the mixed CP-methane hydrate growth rate in NaCl solution is systematically lower than that in pure water for any salt concentrations. Indeed, during hydrates formation in brine, ions are mostly excluded and then accumulate at the vicinity of growing solid hydrate. Therefore, it could locally lower the driving force for hydrate growth. This is called the concentration polarization effect [39].

Finally, the quantity of accumulated salt considerably depends on the kinetic of hydrate formation and the speed of stirring. Consequently, the concentration polarization effect can be reduced by enhancing the mixing to transport salt away from the growing crystal.

3.6 Interfacial effects, surfactants

Hydrate formation kinetics is also deeply related to surface phenomena [143,166–170]. Interfacial tension of liquid-liquid or liquid-gas system plays a crucial role on the mass and heat transfers. Some additives, which affect the interfacial tension, can be used as a promotor while others can be used as an inhibitor for hydrate formation.

It is known that CP is a hydrophobic hydrocarbon. Hence it is immiscible with water. Therefore, complete conversion of water (or CP) into CPH is hard to achieve. This issue can be remedied by adding a small quantity of certain surfactants to the process [68,132,134,135,166]. Of course, it is then difficult to separate fresh water from liquid CP afterward.

Erfani et al. [134] investigated the effects of 14 surfactants and polymers on CPH formation. The results showed that the addition of surfactants can highly decrease the induction time and enhance the hydrate formation rate. Furthermore, Lauryl Alcohol Ethoxylates with 8 ethoxylate groups (LAE8EO), TritonX-100 and Nonyl Phenol ethoxylates with 6 ethoxylate groups (NPE6EO) were found to be the best additives to increase the kinetic of hydrate formation. Erfani et al. [134] demonstrated that surfactants generating oil in water emulsion improved the kinetic of hydrate formation better than those generating water in oil emulsion.

Lo et al. [166] declared that CPH growth rate is higher in presence of sodium dodecyl sulfate (SDS) and dodecyl-trimethylammonium bromide (DTAB) than without surfactant.

Likewise, Karanjkar et al. [130] and Zylyftari et al. [68] reported that Span 80 promotes CPH formation. However, Peixinho et al [75] observed the opposite. They witnessed that addition of surfactant Span 80 (0.0001, 0.01, 0.1% mass) into water, to form water in oil emulsion, decreases kinetic time for hydrate formation. According to them, surfactant Span 80 molecules cover the CP-water interface and inhibit water and CP diffusion. Thus, the CPH formation is prevented. This variation of the influence of Span 80 on kinetics could be attributed to differences in the experimental systems. For instance, Zylyftari et al [68] studied the CPH formation in the hydrate-forming emulsion, while Peixinho et al [75] studied CPH formation in one water drop in CP phase without agitation.

Brown et al [74] reported that the CPH shell thickness is not modified when surfactants are introduced into the system. This study reveals that they have different effects on the growth rate: Dodecylbenzenesulfonic acid at a concentration of 10^{-6} mol/L (DDBSA) and Tween at 10^{-4} mol/L decrease slightly the growth rate, while DDBSA at 10^{-4} mol/L and Tween at 10^{-8} mol/L slightly increase the growth rate.

Delroisse et al. [77] indicated that the average lateral growth of CPH in the presence of 0.1% and 1% of surfactant DA 50 (benzyl-dodecyl-dimethylazanium chloride, $C_{21}H_{38}C_lN$) is about twice lower compared to pure water system.

Furthermore, Zhang et al. [140] indicated that polyvinyl pyrrolidone (PVP) and polyvinylcaprolactam (PVCap) acted as inhibitors on CPH formation. In fact, PVP and PVCap prevented CP diffusion from the bulk to the hydrate surface. This hence decreases the growth rate of CPH. Hobeika et al. [76] showed that, with PVP, PVCap, or vinylpyrrolidone/vinyl-caprolactam copolymer VP/VCap present, the CPH growth rate is much lower compared to pure water. Therefore larger subcooling is required. Moreover, among these three polymers, PVCap was found to be best to prevent hydrate formation.

Dirdal et al. [65] investigated the inhibition efficacy of various of kinetic hydrate inhibitors (KHIs) of CPH formation under atmospheric pressure. Their results exhibited that, in the range of 100-200 ppm, considerable smaller quantities of KHIs are needed to prevent CPH formation than standard gas hydrate formation. Furthermore, Abojaladi et al [138] studied the performance of surfactants (cation, non-ionic, and anion surfactants) as low dosage hydrate inhibitors (LDHI) and anti-agglomerants (AAs) by considering CPH formation. Their results showed that no link was found between hydrophilic-lipophilic balance (HLB) value and AA performance. In addition, it was found that anionic surfactants perform insufficiently, whilst cationic surfactants exposed favorable performances in dispersing hydrate crystals.

To sum up, in desalination, surfactants which promote hydrate formation and/or reduce the induction time such as LAE8EO, TritonX-100, NPE6EO, SDS, DTAB, Span 80, DDBSA and Tween at appropriate concentrations are advantageous. However, since their presence makes the hydrate former difficult to separate after dissociation, their use probably bring more drawbacks than advantages.

3.7 Liquid co-guests influence

Li et al. [139] indicated that the presence of 0.01-0.05% mass THF increases CPH formation rate. Moreover, Mohamed et al. [171] observed that the addition of THF to the CPH system, either with or without surfactants (Span 20, Tween 20), enhances the kinetics of CHP formation. They stated that THF, a highly soluble molecule into water, is a better kinetic additive than Span 20 or Tween 20. Unfortunately, it is difficult to separate THF from water for its reuse in desalination applications. Therefore, use of THF is not recommended in CPH-based desalination processes.

3.8 Other inhibitors

Li et al. [139] elucidated that Rhamnolipid bio-surfactant (product JBR 425) and Methanol inhibit CPH formation. Moreover, Baek *et al.* [51] demonstrated that activated carbon particles act as a kinetic inhibitor for the mixed hydrate of CP and propane. At 1%mass of activated carbon particles, the particle layer covers the whole interface between hydrate formers and water, preventing mass transfer and diffusion. Therefore, hydrate growth is retarded compared to pure mixed hydrate without activated carbon particles.

Finally, Morrissy et al. [141] indicated that free resins (FR), binding resins (BR), and residual asphaltenes (RA) in the crude oil reduce CPH film growth rate with a trend in following order: RAs > BRs > FRs. Above a given concentration threshold, these additive species are suspected to settle at the water/CP interface. Consequently, this prevents the growth of CPH crystals [141].

3.9 Conclusion on kinetics

Table 6 reveals that there have been several methods to increase the hydrate formation rate such as increasing subcooling, quantity of CP, agitation speed, using memory effect, using heterogeneous nucleation by ice or graphite, and addition of appropriate surfactants. Nevertheless, the methods of increasing subcooling and agitation speed consume much more energy than other methods. Moreover, increasing the quantity of CP is also a costly method because the huge quantity of seawater or salt water employed in a real facility. The uses of memory effect and/or heterogeneous nucleation by ice or graphite are probably favorable techniques to improve CPH kinetic due to low cost and operating simplicity. Appropriate surfactants could give the impression of being good method because of their high capability to

enhance kinetics of CPH formation. However, their use is a significant issue in water/CP separation since an emulsion is formed.

4. Physical properties of CPH

Crystal morphology is another important aspect of hydrate-based technologies [148], and of course CPH-based desalination [64]. Indeed, CPH crystal shape strongly influences the kinetics of the formation process and it should be taken into account in designing equipment such as reactors and transportation devices. Adhesion, cohesion, rheology, interfacial tension, yield stress, and shell property are also useful common properties of hydrates. These are essential factors that affect CPH transportation in the process. In this section, morphology and physical properties of CPH in the open literature are classified and presented.

Table 7 provides different properties of CPH in the literature. The following subsections look at different parameters in detail.

Table 7. CPH physical properties studied in the literature

Properties	Citation
Morphology	[42,45,64,71,74–77,87,122,126,127,129,131,171–174]
Adhesion	[42,62,80,175–180]
Cohesion	[74,137,141,175,177,181,182]
Rheology	[68,173,183–185]
Interfacial tension	[68,73,74,76,77,80,122,131,134,166,169,170,175,177,179,181]
Yield stress	[68,172]
Hydrate density	[14,60,76,77]
Wettability	[77,81,123]
Shell property	[74]
Heat of formation	[60,78,130,186,187]
Heat capacity	[186]
Torque	[174]

4.1 Morphology

Hobeika et al. [76] reported that the growth rate and morphology of CPH remarkably depends on subcooling. CPH grow slowly with some large crystals present at low subcooling, while CPH grow quicker with many small crystals under high subcooling. Furthermore, the morphologies of CPH are different when additives like PVP, PVCap, or VP/VCap are present. In this case, CPH particles are thinner, less glassy, and more fragile.

Sakemoto et al. [64] and Kishimoto et al. [87] pointed out that the morphology of the individual CPH crystals in water, seawater and brine at any NaCl concentration are comparable at a similar subcooling. Moreover, the size of the CPH crystals are smaller at higher subcooling [87]. In addition, Mohamed et al. [171] reported that the nature of surfactants affects the morphology of CPH. Delroisse et al. [77] studied the morphology of CPH at different surfactant DA 50 concentrations. Their results showed that at 0.01% mass DA 50, small hairy hydrate crystals with a large quantity of needles and some many-sided shapes were observed. At 0.1 and 1% mass DA 50, smaller hydrate crystals with many-sided, three-sided, and sword-like shaped were observed. This was attributed to differences in the configuration of the surfactant molecules absorbed on hydrate surface, due to differences in surfactant concentration tested.

Mitarai et al [71] elucidated that, with Span surfactant present, the individual CPH crystals had a larger size compared to those in the system without Span surfactant. Their results also indicate that Span has two effects: inhibition of hydrate agglomeration; enhancement of hydrate formation.

Lim et al. [126] showed that adding SDS can modify the CPH hydrate crystal morphology. Indeed, with SDS present, the same length rectangular tree-like or fiber-like crystals were observed from hydrate deposit.

4.2 Adhesion

Aspenes et *al.* [175] investigated adhesion force between CPH and solid surface materials. Their results showed that the force of adhesion depend on the surface materials and the presence of water. Low free energy surface solids lead to the lowest adhesion. The hydrate-solid surface adhesion was more than 10 times stronger than hydrate–hydrate adhesion. Adding petroleum acids declined adhesion, while the presence of water-dissolved oil phase improved adhesion. In addition, water-wet solid surfaces were found to have the strongest adhesion.

Nicholas et al. [62] revealed that adhesion between CPH and carbon steel was found to be significantly weaker than CPH – CPH particles and were also lower than ice – carbon steel. Aman et al. [177] reported that CPH adhesion forces are 5 to 10 times stronger for calcite and quartz minerals than stainless steel, and adhesive forces are strengthened by 3 – 15 times when delaying surface contact time from 10 to 30 seconds. Finally, Aman et al. [176] demonstrated that hydrate adhesion drops significantly with Span 80, polypropylene glycol, or naphthenic acid mixture present in a mineral oil and CP continuous phase.

4.3 Cohesion

Brown et al. [182] observed that, at different temperatures, longer annealing time led to lower cohesive force. Indeed, annealing step disrupts micropores or capillaries in hydrate structures, where free water is transported from the hydrate core to the outer surface. This diminishes the water layer favorable for cohesion.

Aman et al. [181] determined cohesion force for CPH in water, hydrocarbon, and gas bulk phases. Their results showed that cohesion is different in various phases. Cohesion in gas phase is roughly twice and six times stronger than that in the hydrocarbon phase and in the water phase, respectively. Furthermore, Aman et al. [80] reported that cohesion force of the CPH particles is 9.1 ± 2.1 mN/m and 4.3 ± 0.4 mN/m at around 3°C in the gas phase (N_2 and CP vapor) and in the pure liquid CP phase, respectively.

4.4 Interfacial tension

Aman et al. [169] affirmed that the interfacial tension of CPH – water and CPH – CP is 0.32 ± 0.05 mN/m and and 47 ± 5 mN/m, respectively. Brown et al. [74] indicated that the addition of Tween 80 leads to a remarkable drop in interfacial tensions at high concentrations above critical micelle concentration (CMC) in a water bulk phase. Nonetheless, dodecylbenzenesulfonic acid (DDBSA) showed no dependence of interfacial tension under concentrations below the CMC.

Moreover, Delroisse et al. [77] concluded that, in presence of DA 50, the interfacial tension between CPH and water increases while the interfacial tension between CPH and CP diminishes.

4.5 Rheology

In term of CPH rheology, Karanjkar et al. [183] indicated that CPH slurry viscosity is proportional to the water volume fraction. Slurry viscosity decreases (1-3 Pa.s at 8 °C) with increasing of subcooling (below freezing ice temperature). This is explained by ice formation. Indeed, more ice was observed in the CPH slurry system at lower temperatures (higher subcooling) than at higher temperature (lower subcooling), resulting in lower viscosity.

Moreover, at Span 80 concentrations of 0.5-5% (v/v), viscosity was found to be lower due to the accessibility of extra quantity of Span 80 molecules (oil-soluble surfactant) which can adsorb onto the CPH interface and weaken CPH-CPH interactions. Therefore, Span 80 can increase the flowability as an anti-agglomerant at high concentrations.

In addition, when introducing ice to the system to induce hydrate crystallization, Zylyftari et al. [129] observed that the viscosity of the mixture increases faster than by introducing CPH.

Finally, since high viscous hydrate slurry requires much more energy to be transported, methods to reduce viscosity, such as the use of surfactants or especially CPH seeds, are recommended in CPH-based desalination.

4.6 Yield stress

Ahuja et al. [172] determined that the yield stress of CPH slurry rises quickly from 5 Pa to 4600 Pa when increasing the water volume fraction (ϕ) from 16% to 30% above a critical water fraction (ϕ_c) of 15%. A power dependence of the yield stress of CPH and slurry viscosity on water volume fraction was also found, scaling as $(\phi - \phi_c)^{2.5}$.

Zylyftari et al. [68] reported that, at low water conversions (< 27%vol), the yield stress is quite small (10^{-1} Pa). At higher water conversions (42-81%vol), yield stress increases to 100 Pa. It reaches to a maximum of 145 Pa at 81%vol conversion. The behavior of yield stress as a function of the water to CPH conversion exhibits a similar tendency as the viscosity. This also illustrates the effect of capillary bridges between CPH particles. At 81% water conversion, the yield stress is maximum (145 pa), showing the optimal number of capillary bridges and CHP surface required to have the strongest network structure.

4.7 Density

Sloan et al. [14], Delroisse et al [77], Hobeika et al. [76] and Nakajima et al. [60] indicated that CPH density is about 950 to 960 kg/m^3. At standard conditions, this value is between the density of brine (>1000 kg/m^3) and CP (751 kg/m^3). Thus, CPH floats on water and sinks in liquid CP.

4.8 Wettability and shell properties

Delroisse et al. [77] reported that CPH is CP – wettable with surfactant DA 50 present. However, Karanjkar et al. [81] indicated that in the presence of Span 80, CPH is water – wettable. This requires selecting the appropriate surfactants to be used in desalination to optimize hydrate separation from the aqueous and also CP phases.

Brown et al. [74] investigated the effect of surfactants on CPH shell properties. It was found that the addition of DDBSA and Tween 80 changed the CPH properties. Indeed, the CPH shells, with DDBSA and Tween 80 present, require a much lower perforation than for pure CPH. This indicates that adding these surfactants weaken the CPH shell strength.

4.9 Thermodynamic properties

Two thermodynamic parameters including heat of formation and heat capacity have been well reported in literature [60,78,130,186,187]. These two parameters are crucial for the design and optimization of CPH-based desalination [186].

The value of heat of formation (kJ/mole of water) varies according to authors: 4.84 [130,187]; 5.098 [186]; 6.786 [78]. The CPH heat capacity was firstly approximated from the heat capacities of THF and propane hydrate according to He el al. [186] as follows:

$C_P = -124.33+3.2592T+2\times10^{-6}T^2-4\times10^{-9}T^3$ where T is the absolute temperatures (K).

4.10 Torque

The agglomeration phenomena of hydrate crystals are important in hydrate-based desalination since they are related to the transport of hydrate in the desalination process. The torque value is one of the common factors that represent the agglomeration of hydrate [89,138,159,184,188]. Delroisse et al [174] reported that, without biodegradable anti-agglomerant (called AA-LDHI [174]) in a stirred-tank reactor, the torque of CPH increases progressively to 0.3N.m until the agitator stopped at 550 min (approximately 0.7N.m). It is because of the significant increase in

viscosity after the crystallization onset, when CPH crystals agglomerated *via* capillary bridges. In addition of 0.1% AA-LDHI, the torque drops significantly, about ten times. Furthermore, in the presence of AA-LDHI, when CPH crystallization started, the torque grows slightly from 0.025 N.m to 0.035 N.m and then remains nearly constant. The results indicate that the added AA-LDHI disperses CPH particle (average diameter of 380 ± 150 μm [174]) and reduce their agglomeration during crystallization. Consequently, this is expected to facilitate the transport of CPH crystals in desalting processes.

4.11 Conclusion on CPH physical properties

In many cases, adding surfactants modifies morphology and physical properties of CPH in aqueous solution. The choice of appropriate kind and amount of surfactants could be favorable to the improvement of CPH kinetics and transport.

Besides, some issues on the use of surfactants should be prudently considered. Since they are soluble into water, and enhance CP solubility into water, it is very difficult to recover them by a simple physical method as decanting. Indeed, some techniques for removal surfactants from water could be applied such as nano-filtration [189], activated carbon/ultrafiltration hybrid process [190], coagulation [191,192], or constructed-wetland-treatment systems [193]. Bio-surfactants are also a good suggestion for CPH-based desalination since they promote hydrates formation and they are degradable [174,194,195]. However, the use of surfactants still needs more efforts to purify the dissociated water and increases the total operating cost. Therefore, minimizing quantity of the surfactants is one of the requirements for feasible CPH – based salt removal process.

5. Influence of operating conditions on CPH–based desalination efficiency

Gas hydrate formation involves high pressure conditions, and therefore appropriate equipments are required to design a hydrate–based process. Indeed, operating costs could be significantly higher compared to standard processes (distillation, reverse osmosis…). This cost drawback is the reason hydrate-based desalination has not been commercialized yet. As discussed earlier, the use of CP as guest for desalination in combination with other applications, such as gas capture/separation, or cold energy storage (see later in section 6.2), might be advantageous or profitable.

Remember that, with CP, hydrate crystallization occurs at only one bar under normal atmospheric pressure. In addition, CP can be recovered easily after hydrate dissociation since it is not miscible into water. This simplicity is an enormous advantage, and this is probably why CPH-based desalination is still of interest in the scientific community.

Recently, the use of CPH for desalination has been investigated at both laboratory and pilot scales [42,43,69,119,124,186,188,196–198] considering three main concerns: yield of dissociated water from CPH, water conversion to hydrate, and salt removal efficiency. The effects of mentioned considerations on CPH-based desalination process are detailed in Table 8.

Table 8. Effect of various considerations on CPH-based desalination process

Considerations	Yield of dissociated water	Water conversion to hydrate	Salt removal efficiency	Citation
Quantity of CP:				
+ CP concentration in				
1 – 5 mol% range: ↑	NA	↑	NA	[69]
0.9 – 2.3 mol% range: ↑	NA	↑	Fluctuated	[42]
+ Water cut in				
20 – 60 vol % range: ↑	↑	NA	↓	[119]
70 - 90 vol % range: ↑	↓	NA	↑	[119]
Agitation:				
300 – 500 rpm range: ↑	↑	NA	↓	[119]
300 – 600 rpm range: ↑	NA	↑	NA	[124,197]
600 rpm	NA	NA	↑	[43]
Operating temperature:				
0.95 – 3.95°C range: ↑	↓	NA	↑	[119]
-2° – 2°C range: ↑	NA	↓	NA	[124,197]
0.4 – 2.4 °C range: ↑	NA	↓	↓	[42]
Salinity:				
3 – 5% mass NaCl range: ↑	↓	NA	↑	[119]

0.17 – 5% mass NaCl range: ↑	NA	↓	NA	[124,197]
Use of graphite	↑	NA	↑	[43]
Use of filtering	NA	NA	↑	[69,124,196,197]
Use of centrifuging	NA	NA	↑	[69]
Use of washing By 3.5 % mass brine water	↑	NA	↑	[119]
By fresh water	↑	NA	↑	[119]
By fresh water	NA	NA	↑	[69,196]
By DI water	NA	NA	↑	[124,188,197]
By filtered water	NA	NA	↑	[124,197]
Ratio of washing water/dissociated water (g/g) 0.1 – 0.5 range: ↑	Fluctuated	NA	↑	[119]
0.5 – 1.2 range: ↑	Fluctuated	NA	Fluctuated	[119]
0.02 – 0.03 range: ↑	NA	NA	↑	[69]
0.03-0.05 range: ↑	NA	NA	↓	[69]
0 – 0.035 range: ↑	NA	NA	↑	[196]
0.035 – 0.05 range: ↑	NA	NA	↓	[196]
Use of sweating	NA	NA	↑	[69]
Use of gravitational separating	NA	NA	↑	[124,197]
Use of spray injecting	NA	↑	NA	[124,197]
Use of tube injecting	NA	↑	NA	[124,197]

where ↑: increase; ↓: decrease, NA: Not Acknowledge

Removal efficiency, yield of dissociated water, water conversion to hydrate, ratio of washing water/dissociated water (g/g), CP concentration, and water cut were calculated as follows:

$$\text{Yield of dissociated water} = \frac{m_l}{m_o} \times 100\% \text{ or } = \frac{V_l}{V_o} \times 100\% \quad (1)$$

where m_o/V_o are the mass/volume of initial salt solution, and m_1/V_1 are the mass/volume of melted water [43,119].

$$\text{Water conversion to hydrate} = \frac{m_c}{m_o} \times 100\% \quad (2)$$

where m_c is the mass of water converted to hydrates [42,69,124,196,197].

$$\text{Salt removal efficiency} = \frac{C_0 - C_1}{C_0} \times 100\% \quad (3)$$

where C_0 is weight percent of NaCl in prepared brine and C_1 is that in dissociated water [42,43,69,119,124,196,197].

$$\text{Ratio of washing water/dissociated water} = \frac{m_2}{m_1} \times 100\% \quad (4)$$

where m_2 is the mass of water used for washing [119]

$$\text{CP concentration} = \frac{n_{CP}}{n_{brine}} \times 100\% \quad (5)$$

where n_{CP} is the mole number of CP and n_{brine} is the mole number of initially prepared brine [42,69]. This is somewhat related to another parameter in the literature, the "Water cut".

$$\text{Water cut} = \frac{V_{brine}}{V_{brine} + V_{CP}} \times 100\% \quad (6)$$

where V_{brine} is the volume of initially prepared brine and V_{CP} is the volume of CP [119]

In the next sections, some details are provided to explain the effects of some considerations on the CPH-based desalination process.

5.1 Quantity of CP.

Water cut can be used to indicate quantity of CP as described by Equation (6). When water cut increases, quantity of CP then decreases because these two parameters are inversely proportional to each other.

Table 8 illustrates that the water conversion into hydrate increases by raising the CP concentration in the system [42,69]. Also, the salt removal efficiency varies irregularly from less than 70% to close to 90% when increasing CP concentration from 0.9 to 2.3 mol % [42].

Moreover, the water cut can affect the yield of dissociated water and the salt removal efficiency differently [119]. The yield of dissociated water first augments significantly with water cut from 20% to 60% while the removal efficiency declines inappreciably. When the water cut is in 60% - 90% range, the yield tends to lessen considerably while the removal efficiency is slightly improved. To summarize, the removal salt efficiency for different water cut varies from 75% to 85%. This demonstrates that, compared to high water cut systems (>80 vol% water or <5 mol%

CP [42,69]), extra CP addition in brine could considerably improve the yield of dissociated water while the removal efficiency undergoes a relatively minor change.

The effect of CP quantity on the hydrate formation rate is described in elsewhere [42,119,126,127]. It was found that excess CP can increase notably the kinetics of hydrate formation, and hence the conversion of water to hydrate and the yield of dissociated water.

5.2 Agitation

Change in flow condition, or shear rate, is observed using various stirring rates. This leads to different mass and heat transfer rates in the system. Table 8 shows that boosting the agitation rate promotes water conversion and yield of dissociated water, as examined by different authors [39,43,60,70,119,124,125,197]. However, this comes with a decrease in salt removal efficiency [119]. Indeed, higher agitation rates may enhance the reaction kinetic and hence cause formation of smaller hydrate crystals with larger specific surface area. As a hydrate surface is hydrophilic, more salt ions tend to attach on the crystal surfaces, leading to a difficult separation of brine from hydrate [119].

The way CP is introduced into a system can also change the hydrate formation kinetics. Xu et al [124,197] declared that, by using the CP spray injection method, higher water conversion can be achieved, due to the smaller CP droplets created by the spray injection. However, a pump is hence needed for CP injection in this case, thus more energy is required.

5.3 Operating temperature

Table 8 indicates that the operating temperature affects strongly water conversion to hydrate, yield of dissociated water, and removal efficiency. At higher operating temperature, the hydrate formation rate decreases due to decrease in the driving force (here subcooling). Thus, both water conversion and yield of dissociated water are reduced with higher operating temperature [42,119,124,197].

However, two different observations in purification efficiency when increasing operating temperature were reported by Beak et.[42] and Lv et al.[119].

One the first hand, Beak et al. elucidated that, at operating temperature of 2.4°C, the purification is less efficient than at 0.4°C. This is attributed to higher attractive force between CPH particles. Certainly, adhesion forces between CPH particles increase linearly with rising temperature [199].

Thus, at higher temperatures, growing CPH crystals adhere to each other in a stronger framework than at lower temperatures. Consequently, more brine is trapped between CPH crystals, and a post-treatment method, such as centrifuging, is required.

One the second hand, Lv et al.[119] showed that the salt removal efficiency improves when increasing operating temperature from 0.95 to 3.95°C (or 274.1 – 277.1K). It was found that the residual salinity is likely to be strongly related to the shapes and size of hydrate crystals. Kishimoto et al. [87] specified that the size of the hydrate crystals diminished with subcooling increase.

Moreover, by using the FBRM probe, Lv et al.[119] indicated that the median chord length of CPH particles after 8h formation at 0.95 °C (274.1 K) is 22.16 μm, while, particles formed at 3.95°C (277.1 K) under the same other conditions exhibited a median chord length of 34.15 μm. Thus, it was supposed that at higher operating temperature (or lower subcooling), hydrate particles are bigger with a smaller specific surface area favorable to salt removal [119].

To sum up, in order to clarify the effect of operating temperature on the purification efficiency, more data at a varied range of operating temperature and salt concentration would be needed.

5.4 Salinity

Table 8 shows that the salt removal efficiency increases slightly with the salinity increase, while both water conversion to hydrate and yield of dissociated water appear to decrease considerably [119,124,197]. Indeed, when there is uptake in salt concentration, the driving force for hydrate formation decreases [28,119,124,197]. This reduces the CPH formation rate [39,68,87,119]. As a result, less water converts into hydrate under higher salt concentrations.

Moreover, an enhancement in purification efficiency at high operating temperatures can be attributed the CPH crystals size change. Indeed, the hydrate formation kinetics decreases as salt concentration increases [39,68,87,119]. Thus, bigger hydrate particles with a smaller specific area are likely to form. Consequently, there is less brine trapped between CPH crystals.

5.5. Solid additives

As aforementioned, the addition of some solid additives can promote CHP formation [43,61,75,129,130]. Moreover, Li et al [43] reported that the addition of graphite not only enhances CPH formation but also boosts the salt removal efficiency. They indicated that the

surface functional groups of graphite improve both hydrate nucleation and growth of CPH. Moreover, the hydrophobic surfaces of graphite could inhibit hydrate aggregation and make hydrate crystal particles more porous. Consequently, the trapped salt ions can be removed more easily by centrifuging process, thus increasing the salt removal efficiency [43]. In addition, in presence of graphite, the prolongation of hydrate formation improved the desalting efficiency [43]. The hydrophobic behavior of graphite is believed to play a crucial role in this improvement [43]. These findings present interesting perspectives for the use of graphite or carbon material surfaced in the development of CPH-base desalination techniques.

5.6 Post-treatment methods

In order to remove salts trapped onto the hydrate surfaces, some post-treatment methods are introduced, such as filtration, centrifuging, sweating, gravitational separation, and washing. Several studies concluded that all these techniques can enhance profoundly the salt removal efficiency [69,119,124,196,197].

About 60-63% of NaCl from the feed solution was removed after CPH formation with only vacuum filtration [69,196]. It means that the treated water still contained a high level of NaCl. Obviously, this level of water purification is insufficient for desalination, so further post-treatments are needed.

Han et al. [69] demonstrated that centrifuging can enhance salt removal efficiency up to 96%. However, centrifuging is very expensive for mass treatment. Sweating by melting the impure zone over time can be a potential process to enhance salt removal. Nonetheless, it reduces the quantity of water retrieved. Moreover, this process is time consuming, hence an optimal time should be determined for the sweating of CPH crystal [69].

Washing is also an effective approach to enhance salt removal [69,119,124,196,197]. The source of the wash can be fresh, DI water, filtered water, or even brine water. The effect of washing water/produced water ratio on salt removal was remarkable. Han et al. [69,196] indicated that the optimal ratio of washing water/ produced water is approximately 0.03 (g/g) with a salt removal efficiency above 90%. Lv et al. [119] suggested that this value should be 0.5 (g/g) in order to remove enough salt from CPH crystals. However, this value is extremely high for industrial scales. Therefore, more investigation is required to optimize this ratio in order to meet the requirement of water purification and reduce the costs of desalination process.

Finally, forthcoming research should combine optimization of both kinetics of CPH formation and the salt removal efficiency [119]. Post-treatment methods may include filtration or pelletizing (squeezing) at first step [11,13] in order to facilitate CPH separation from aqueous solution and transportation to dissociation devices. Furthermore, to meet potable water standards, several existing technologies like washing and sweating are needed to remove entrapped salt ions on the crystal surfaces. Of course, optimizations on these technologies are also required for the economy feasibility of the desalting process.

6. Comparison to other desalination technologies

6.1 Comparison to traditional technologies

Other processes such as multi-stage flash distillation (MSF), multiple-effect distillation (MED), solar thermal distillation (SD), freezing, reverse osmosis (RO), ecletro-dyalysis (ED), ion-exchange desalination (IE), and adsorption have been investigated, and industrially used, for seawater desalination [6,10,27,36,118,200–214].

Table 9 presents a comparison between diverse technologies based on four criteria: Thermal Energy consumption, electrical energy consumption, production cost, and product water salinity. Also, note that, in the case of clathrates, different formers can be used. Therefore, there are other opportunities than CPH to consider when discussing hydrate-based desalination. Consequently, a short comparison between different clathrate formers will be presented in the next section. Table 9 illustrate of what can be expected with other clathrate than CPH.

In term of purification level, MSF, MED, RO, adsorption, or clathrate hydrate technique can produce water with salinity lower than 10 ppm. Of course, this value varies according to the procedure and technology. For hydrate-based desalination, Subramani et al. [10] estimated that the technique can reach 100% salt removal in theory. However, such quality should not be expected. For instance, McCormack et al [32] obtained fresh water with a salinity of 100 ppm by using HCFC 141b (Dichloromonofluoroethane – CCl_2FCH_3) clathrates. In a patent, Mottet [198] evaluates that the salinity for the treated water via CPH crystallization to be 1000 ppm. By using a new batch-wise displacement washing technique in CPH-based desalting process, Cai et al [188] obtained fresh water with a salinity less than 10 ppm (<0.001% mass). Accordingly, in other efforts, Han et al. [69,196] and Lv et al. [119] indicated that CPH-based desalination

technology can produce water with a salinity from 700-4400 ppm. Recently, Xu et al [197] and Li et al [43] reported values of 700 ppm and 4008 ppm, respectively.

Note that, according to World Health Organization (WHO), the palatability of water with a total dissolved solids (TDS) level less than 600 mg/l is generally considered to be good; drinking-water becomes significantly and increasingly unpalatable at TDS levels greater than 1000 mg/l [215]. Remember that seawater has an average of 35000 ppm TDS [210,216]. The high TDS value (here salinity) of product water via CPH-based desalination is strongly related to the salts trapped in the hydrate crystals [6,10,27,36,118,200–214]. This requires efforts on post-treatment process to completely remove trapped salt and therefore achieve product water with quality that meets the WHO drinking-water criterions.

Table 9. A comparison in energy consumption, production cost and product water quality between desalination technologies

Desalination technology	Thermal energy consumption (kWh/m^3)	Electrical energy consumption (kWh/m^3)	Production cost ($\$/m^3$)	Water salinity (ppm)
MSF	52.78-78.33[200]	15.83-23.5 [200]	0.52-1.75 [200][217] 1.0785 [218] 0.77-1.64 [207]	10 [200]
MED	40.28-63.89 [200]	12.2-19.1 [200]	0.52 -8.0 [200] 0.87-1.95 [207]	10 [200]
SD	0 [200,210]	0 [200,210]	1.3-6.5 [200] 3.9 [210]	80 [210]
Freezing	*	9-11[219]	0.93 [219,220]	100 [210]
RO	4.1 [5]	4.0 [5] 3-7 [221] 8.2-9.0 [207]	0.85 [206,211] 0.45-1.72 [200] 0.64-0.76 [207]	35 [5,205] 400-500 [200] 10 [210]
ED	*	2.64-5.5 [200]	0.6-1.05 [200]	150-500 [200]
IE	*	1.1 [210] 0.29-1.04 [222]	1.05 [210]	13 [210]
Adsorption	*	1.38	0.18 [207]	7.54 [207]

		[10,204,207]		10 [210] Up to 100% rejection [10]
CPH	*	0.35 [186]	*	< 10 [184] 1000 [198] 700-4400 [69,119,196] 4008 [43] 700 [197]
Other Clathrates				
HCFC 141b hydrates	*	1.58 [32,210]	0.63 [32,210] 0.46-0.52 [10]	100 [32,210] Up to 100% rejection [10]
Propane hydrates	*	0.60-0.84 [35]	2.76 [211] 1.11 [223]	100-500 [224]
CO_2 hydrates	*	*	*	7665 [11] 1100 [13] 23270 [90]
CO_2+CP hydrates	*	*	*	8055 [90]

* Not Acknowledge

In terms of energy consumption, Table 9 indicates that clathrate hydrate, adsorption, SD, or IE technology require the lowest amount of energy (< 2kWh/m^3), whilst MSF, MED, and Freezing consume an energy almost more than 10 kWh/m^3. The lower energy required in clathrate techniques compared others is related to its low phase change enthalpy. As clarified in Table 10, HCFC 141b hydrate or CPH requires a smaller energies (5.74 or 4.84 kJ/mol water, respectively) compared to freezing water (6.02 kJ/mol) or water evaporation (40.7 kJ/mol) [69,130,187].

Table 9 also displays that the production cost for adsorption and clathrate hydrate is much smaller than MSF, SD, freezing, and IE technologies. For instance, production costs for HCFC 141b and propane hydrates are less than 0.6 \$/m^3 and 1.11 \$/m^3, respectively. Otherwise, it is between 0.6 and 1.95 \$/m^3 for RO, MED, and ED technologies.

The above assessments indicate that clathrate hydrate and adsorption techniques could be able to produce high quality fresh water with a low energy consumption (< 2kWh/m^3) and minimum operating cost (less or around 0.6-1.11 \$/m^3). Thus, both clathrate hydrate and adsorption technologies could be promissing technologies after proper development compared to conventional processes.

However, there are some strong drawbacks concerning the adsorption technique [10]: it requires waste heat or renewable energy source for cost-effective desalination. Robustness of silica gel adsorber beds is still not known. Data are available only for demonstration-scale projects. Thus, this technique still requires more study.

6.2 Comparison between Clathrate formers for hydrate-based process

Concerning hydrate-based approach, the kind of former is crucial. It is one of the most important factors in hydrate-based desalination since the operating conditions strongly depend on the guest molecules. With a possibility to form hydrate at temperature above 0°C from seawater, CHFC 141B has been studied for desalination in the last few decades [32,33,225]. However, CHFC 141B has a solubility of 350mg/l at 15.6^{o}C [32] higher than that for CP (156mg/l at 20°C) [28,46]. Moreover, HCFC R141B is also very volatile (boiling point of 32.2°C) [32]. This leads to an ozone-depletion problem when released into the atmosphere [226]. International concern over relatively high global warming potential of HCFC has caused some European countries to abandon it for many applications such as refrigerants or as a cleaning agent [226]. HCFC compounds, such as R141b, are hence restricted by current environmental regulations and are no longer practical candidates for a hydrate desalination process, despite their ease of use [33].
Recently, He et al [35,227], Nambiar et al [228], and Chong et al [223], proposed a propane-hydrate based desalination process using LNG cold energy. When compared to MSF, RO, and freezing techniques, Babu et al [229] demonstrated that this technology (the HyDesal process) can be economically attractive. As shown in Table 9, this process requires a remarkably low energy (0.60-0.84 kWh/m^3) compared to others. The cost of potable water was found to be approximately \$1.11/m3 with LNG cold energy integration [223]. LNG cold energy from the LNG regasification terminals replaces the external refrigeration cycle. Of course, this

desalination technique still needs a stable LNG cold energy source. High-pressure devices (0.4 Mpa) are also required to form propane hydrate. Lastly, it should be noticed that LNG and propane are flammable and explosive gases at high pressure. Thus, although its economic feasibility, also estimated by Chong et al [223], an industrial-scale testing of this process is not yet available.

In addition, Table 10 shows that CPH have a lower phase change enthalpy compared to CHFC 141B hydrate, CO_2 hydrate, and propane hydrate. The energy required for CPH-based desalination is hence likely less than for CHFC 141B hydrate, CO_2 hydrate, or propane hydrate based desalination.

Newly, He et al [186] investigated the techno-economic of CPH-based desalination utilizing LNG cold energy. Their results indicate that CPH-based desalination technique requires a specific energy consumption of 0.35 kWh/m^3, which is 58% lower than desalting technology utilizing propane hydrates. The Fixed Capital Investment (FCI) of the CPH-based desalination process was estimated to be $6,113,751 (for 0.75 m^3/h of pure water) which is again lower than with propane hydrates ($ 9.6 million for 1.3 m^3/h of pure water [223]). Moreover, the FCI augments from $6,113,751 to $9,559,668 when decreasing the CPH formation temperature from 277.15 K to 273.15 K. Finally, He et al [186] stated that the escalation of the water recovery rate of the CPH can lead to a decline in the SEC and FCI, and to a rise in the pure water flow rate and exergy efficiency. Consequently, improving the water recovery rate of CPH is crucial to enable fresh water production from this technique.

Furthermore, based on the fact that CPH-based desalination requires relatively low temperatures (less than 7°C) for hydrate nucleation and growth, this desalting technique would be more cost-effective if we can use the low temperature of actual seawater instead of utilizing a cryostat. For that purpose, Li et al [43] worked with actual seawater in winter at -10°C. Their results show that the crystallization occurred rapidly over 7h, with a salt removal efficiency of 70% and a water conversation rate of 56%. This indicates one more time the economy feasibility of CPH-based desalting technique when utilizing cold seawater.

Table 10. Latent heat of phase change of several techniques in desalination

Method of desalination	Latent heat of phase change, kJ/mol	Citation
CPH	4.84	[69,130,187]
CO_2 hydrates	57.7±1.8 to 63.6±1.8	[230]
	53.29	[231]
	66.8	[232]
Propane hydrates	27 ±0.33	[233]
Mixed hydrate CP + C_3H_8	2.23	[51]
Mixed hydrate CP + CH_4	131.70 – 121.74	[41]
Form R141 b hydrate	6.19	[225,234]
	5.74	[32]
Freezing water	6.02	[69]
Water distillation	40.7	[69]

7 Example of CPH technological approach

Based on the literature, hydrate-based desalination requires a relative low energy and it is theoretically more competitive economically than other standard processes (distillation, freezing, and RO technologies). To apply that at a commercial and industrial scale, there are still various challenges that need to be addressed. One of the most difficult trials concerns the improvement of two crucial limiting factors: salt removal efficiency and water to hydrate conversion. As detailed in Table 8, these two parameters are usually inversely proportional to each other. There is a need to investigate the best method to transport CPH after formation. Filtration and pelletizing seem to be appropriate to facilitate this transportation step. A washing method is necessary to enhance the salt removal capacity. However, improving the ratio of washing water/dissociated water is also required to make this process economical feasible.

Utilizing LNG cold energy during the regasification process in the LNG regasification terminals for CPH-based desalination is one of the promising approaches to minimize the energy consumption and hence Strengthen Energy-Water Nexus [186]. Of course, this technique requires more experimental explorations before commercial readily-available in the freshwater production industry.

Furthermore, the idea of combining CO_2 capture and desalination can be advantageous when a hydrate mixture of CO_2 + CP is used. Indeed, merging two energy demanding processes can optimize energy use [23,90,92]. However, this procedure is more complicated with the added requirements of higher pressure equipment.

To recap, based on the analysis of all of the articles reviewed, a diagram of CPH-based desalination, with all proposed required steps and apparatus, is proposed in Figure 4.

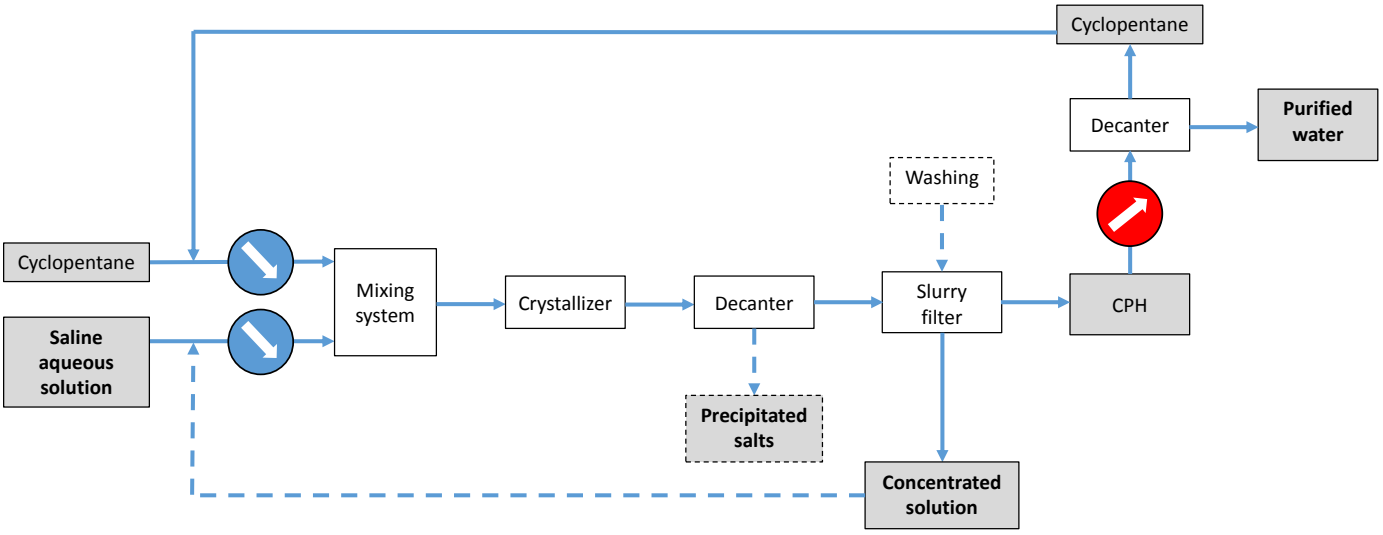

Figure 4. CPH-based desalination process diagram (inspired by [198])

Figure 4 presents a continuous system of water treatment. A mixing system is fed with both cooled CP and saline solution. This mixer, also called an emulsifier is critical to design as it governs the size of the CP droplets in water. The second piece of equipment is crystallizer, where the formation of CPH occurs. Since this is a continuous process; there is no induction time to consider. However, the residence time to complete hydrate formation in the crystallizer is optimized based on the device configuration design in order to reduce the process capital cost.

The slurry is then transferred to a decanter, allowing the growth of hydrate particles and the separation of different phases, notably the possible precipitation of the salts. Then, the slurry filter separates CPH and a concentrated solution. This concentrated solution is waste. However it can be partially re-injected to the mixing system if the aim is to produce saturated solution and precipitated salts. CPH crystals are melted with a heat exchanger and are introduced in a decanter allowing the separation of the CP (on the top) and purified water (on the bottom). The CP is then re-used at the beginning of the process in a closed loop.

A washing step can be also added to the slurry filter. This drives out the concentrated solution trapped between CPH particles. Nonetheless, a less concentrated solution is required. This can be the initial saline aqueous solution or a fraction of the purified water, depending on the rate of purification expected. Although by using a fraction of purified water, while a better purification rate can be obtained, unfortunately the yield of the system decreases.

As seen on figure 4, there are cooling and heating systems in the process. An optimization by energy recovery between the two types of heat exchangers could be considered in order to reduce the energy consumption still further.

From a technological point of view, this flow diagram summarizing all required steps and apparatus for a CPH based desalination process is inspired by the one proposed by BGH Company (France) [198].

According to Mottet [194], here are some advantages to this process:

- CPH can act as both a water purifier and a concentrator of dissolved materials (salts). Interestingly, Ho-van et al [88] reported the precipitation of salts (6% mass Na_2SO_4 at less than 5.3°C) during CPH crystallization. As solid materials, the precipitated salts can be then removed easily by a physical method since their high density compared to others (CPH, CP, brine).
- This is a “no discharge method”, since simultaneous production valorized salts and pure water
- High yield, more than 95%
- This technique can treat highly-salty water (impossible for RO method).
- No pressure requirement, and reasonable operating temperature from -20°C to 7°C

- Less energy consumed than both evaporation and Ice EFC (Eutectic Freeze Crystallization) methods.
- This method is technically more reliable than the Ice EFC as the crystallization of water is internal and direct when CP is added.
- This is a continuous process

Obviously, before hydrate desalination becomes a practical commercial technology, the vital issues of controlled hydrate nucleation, formation rate, phase properties, amount of entrapped salt and its removal efficiency must be thoroughly understood and optimized [33]. As aforementioned, CPH has been recently studied in terms of thermodynamic, kinetic, and phase properties. A relatively sufficient database of CPH for desalination is now available in the literature as provided in this present review.

8 Conclusions

Numerous investigations have been being conducted on CPH for decades. Records on thermodynamic, kinetic, phase properties, and use of CPH for desalination were presented. A comparison between CPH based desalination and other techniques has also been provided. After analyzing vital factors such as energy consumption, product water quality, and economy of desalination plant, conclusions show that Clathrate hydrates present potential for new desalination technique. The use of CP as hydrate former is a promising idea, supported by recent researches in that field. While hydrate technology has not been yet fully developed in the industry, the combination of water desalination to other applications, such as cold energy storage, or even gas separation and storage, makes it again an encouraging idea compared to other competing technologies like distillation, freezing, and reverse osmosis. Of course, other clathrates formers, instead or in addition to CP molecule, could be more suitable for future water treatment applications. However, a diagram of CPH based salt removed has been suggested to illustrate future directions. Finally, some challenges, such as the best economic compromise between salt efficiency and water-to-hydrate conversion need to be addressed before industrial development and implantation.

References

[1] M. Pedro-Monzonís, A. Solera, J. Ferrer, T. Estrela, J. Paredes-Arquiola, A review of water scarcity and drought indexes in water resources planning and management, J. Hydrol. 527 (2015) 482–493. doi:10.1016/j.jhydrol.2015.05.003.

[2] S. Lu, X. Zhang, H. Bao, M. Skitmore, Review of social water cycle research in a changing environment, Renew. Sustain. Energy Rev. 63 (2016) 132–140. doi:10.1016/j.rser.2016.04.071.

[3] K. Watkins, Human Development Report 2006 - Beyond scarcity: Power, poverty and the global water crisis, 2006. doi:10.1016/S1352-0237(02)00387-8.

[4] M.A. Montgomery, M. Elimelech, Water And Sanitation in Developing Countries: Including Health in the Equation, Environ. Sci. Technol. 41 (2007) 17–24. doi:10.1021/es072435t.

[5] U. Caldera, D. Bogdanov, S. Afanasyeva, C. Breyer, Role of Seawater Desalination in the Management of an Integrated Water and 100% Renewable Energy Based Power Sector in Saudi Arabia, Water. 10 (2017) 3. doi:10.3390/w10010003.

[6] A.D. Khawaji, I.K. Kutubkhanah, J.M. Wie, Advances in seawater desalination technologies, Desalination. 221 (2008) 47–69. doi:10.1016/j.desal.2007.01.067.

[7] K.W. Lawson, D.R. Lloyd, Membrane distillation, J. Memb. Sci. (1997) 1–25. doi:10.1016/S0376-7388(96)00236-0.

[8] P. Wang, T.S. Chung, A conceptual demonstration of freeze desalination-membrane distillation (FD-MD) hybrid desalination process utilizing liquefied natural gas (LNG) cold energy, Water Res. 46 (2012) 4037–4052. doi:10.1016/j.watres.2012.04.042.

[9] O.K. Buros, The U.S.A.I.D. Desalination Manual, International Desalination and Environmental Association, 1980.

[10] A. Subramani, J.G. Jacangelo, Emerging desalination technologies for water treatment: A critical review, Water Res. 75 (2015) 164–187. doi:10.1016/j.watres.2015.02.032.

[11] K. nam Park, S.Y. Hong, J.W. Lee, K.C. Kang, Y.C. Lee, M.G. Ha, J.D. Lee, A new apparatus for seawater desalination by gas hydrate process and removal characteristics of dissolved minerals (Na^+, Mg^{2+}, Ca^{2+}, K^+, B^{3+}), Desalination. 274 (2011) 91–96. doi:10.1016/j.desal.2011.01.084.

[12] H. Lee, H. Ryu, J.-H. Lim, J.-O. Kim, J. Dong Lee, S. Kim, An optimal design approach

of gas hydrate and reverse osmosis hybrid system for seawater desalination, Desalin. Water Treat. 57 (2016) 9009–9017. doi:10.1080/19443994.2015.1049405.

[13] K.C. Kang, S.Y. Hong, S.J. Cho, D.H. Kim, J.D. Lee, Evaluation of Desalination by Nanostructured Hydrate Formation and Pellet Production Process, J. Nanosci. Nanotechnol. 17 (2017) 4059–4062. doi:10.1166/jnn.2017.13383.

[14] Sloan ED, Koh CA, Clathrate hydrates of natural gases, Third edition. CRC Press, FL: Boca Raton, 2008.

[15] H. Mimachi, S. Takeya, A. Yoneyama, K. Hyodo, T. Takeda, Y. Gotoh, T. Murayama, Natural gas storage and transportation within gas hydrate of smaller particle: Size dependence of self-preservation phenomenon of natural gas hydrate, Chem. Eng. Sci. 118 (2014) 208–213. doi:10.1016/j.ces.2014.07.050.

[16] Z.G. Sun, R. Wang, R. Ma, K. Guo, S. Fan, Natural gas storage in hydrates with the presence of promoters, Energy Convers. Manag. 44 (2003) 2733–2742. doi:10.1016/S0196-8904(03)00048-7.

[17] A. Burnol, I. Thinon, L. Ruffine, J.M. Herri, Influence of impurities (nitrogen and methane) on the CO_2 storage capacity as sediment-hosted gas hydrates - Application in the area of the Celtic Sea and the Bay of Biscay, Int. J. Greenh. Gas Control. 35 (2015) 96–109. doi:10.1016/j.ijggc.2015.01.018.

[18] H.P. Veluswamy, R. Kumar, P. Linga, Hydrogen storage in clathrate hydrates: Current state of the art and future directions, Appl. Energy. 122 (2014) 112–132. doi:10.1016/j.apenergy.2014.01.063.

[19] N.H. Duc, F. Chauvy, J.M. Herri, CO_2 capture by hydrate crystallization - A potential solution for gas emission of steelmaking industry, Energy Convers. Manag. 48 (2007) 1313–1322. doi:10.1016/j.enconman.2006.09.024.

[20] P.J. Herslund, K. Thomsen, J. Abildskov, N. von Solms, A. Galfré, P. Brântuas, M. Kwaterski, J.M. Herri, Thermodynamic promotion of carbon dioxide-clathrate hydrate formation by tetrahydrofuran, cyclopentane and their mixtures, Int. J. Greenh. Gas Control. 17 (2013) 397–410. doi:10.1016/j.ijggc.2013.05.022.

[21] Z. Taheri, M.R. Shabani, K. Nazari, A. Mehdizaheh, Natural gas transportation and storage by hydrate technology: Iran case study, J. Nat. Gas Sci. Eng. 21 (2014) 846–849. doi:10.1016/j.jngse.2014.09.026.

[22] J.-M. Herri, A. Bouchemoua, M. Kwaterski, P. Brântuas, A. Galfré, B. Bouillot, J. Douzet, Y. Ouabbas, A. Cameirao, Enhanced Selectivity of the Separation of CO_2 from N_2 during Crystallization of Semi-Clathrates from Quaternary Ammonium Solutions, Oil Gas Sci. Technol. – Rev. d'IFP Energies Nouv. 69 (2014) 947–968. doi:10.2516/ogst/2013201.

[23] P. Babu, P. Linga, R. Kumar, P. Englezos, A review of the hydrate based gas separation (HBGS) process forcarbon dioxide pre-combustion capture, Energy. 85 (2015) 261–279. doi:10.1016/j.energy.2015.03.103.

[24] M. Darbouret, M. Cournil, J.M. Herri, Rheological study of TBAB hydrate slurries as secondary two-phase refrigerants, Int. J. Refrig. 28 (2005) 663–671. doi:10.1016/j.ijrefrig.2005.01.002.

[25] J. Douzet, M. Kwaterski, A. Lallemand, F. Chauvy, D. Flick, J.M. Herri, Prototyping of a real size air-conditioning system using a tetra-n-butylammonium bromide semiclathrate hydrate slurry as secondary two-phase refrigerant - Experimental investigations and modelling, Int. J. Refrig. 36 (2013) 1616–1631. doi:10.1016/j.ijrefrig.2013.04.015.

[26] H. Ogoshi, S. Takao, Air-Conditioning System Using Clathrate Hydrate Slurry, JFE Tech. Rep. 3 (2004) 1–5.

[27] H. Fakharian, H. Ganji, A. Naderifar, Desalination of high salinity produced water using natural gas hydrate, J. Taiwan Inst. Chem. Eng. 72 (2017) 157–162. doi:10.1016/j.jtice.2017.01.025.

[28] S. Ho-Van, B. Bouillot, J. Douzet, S. Maghsoodloo, J.-M. Herri, Experimental Measurement and Thermodynamic Modeling of Cyclopentane Hydrates with NaCl, KCl, $CaCl_2$ or NaCl-KCl Present, AIChE. J. 6 (2018) 2207-2218. doi:10.1002/aic.16067.

[29] S.L. Colten, F.S. Lin, T.C. Tsao, S.A. Stern, A.J. Barduhn, Hydrolysis losses in the hydrate desalination process: rate measurements and economic analysis, Desalination. 11 (1972) 31–59. doi:10.1016/S0011-9164(00)84047-3.

[30] J. Sugi, S. Saito, Concentration and demineralization of sea water by the hydrate process, Desalination. 3 (1967) 27–31. doi:10.1016/S0011-9164(00)84021-7.

[31] R.A. McCormack, N.G. A. Build and operate clathrate desalination pilot plant, U.S. Dept. of the Interior, Bureau of Reclamation, 1998.

[32] R.A. McCormack, R.K. Andersen, Clathrate desalination plant preliminary research study, U.S. Dept. of the Interior, Bureau of Reclamation, 1995.

[33] R.W. Bradshaw, D.E. Dedrick, B.A. Simmons, J.A. Great- house, R.T. Cygan, E.H. Majzoub, Desalination Utilizing Clathrate Hydrates, Sandia National Laboratories, California, 2008.

[34] M.D. Max, Hydrate desalination for water purification, US 6991722 B2, 2006.

[35] T. He, S.K. Nair, P. Babu, P. Linga, I.A. Karimi, A novel conceptual design of hydrate based desalination (HyDesal) process by utilizing LNG cold energy, Appl. Energy. 222 (2018) 13–24. doi:10.1016/j.apenergy.2018.04.006.

[36] P. Englezos, The Freeze Concentration Process and its Applications, Dev. Chem. Eng. Miner. Process. 2 (1994) 3–15. doi:10.1002/apj.5500020102.

[37] P. Babu, R. Kumar, P. Linga, Unusual behavior of propane as a co-guest during hydrate formation in silica sand: Potential application to seawater desalination and carbon dioxide capture, Chem. Eng. Sci. 117 (2014) 342–351. doi:10.1016/j.ces.2014.06.044.

[38] A.J. Barduhn, H.E. Towlson, Y.C. Hu, The properties of some new gas hydrates and their use in demineralizing sea water, AIChE J. 8 (1962) 176–183. doi:10.1002/aic.690080210.

[39] L. Cai, B.A. Pethica, P.G. Debenedetti, S. Sundaresan, Formation of cyclopentane methane binary clathrate hydrate in brine solutions, Chem. Eng. Sci. 141 (2016) 125–132. doi:10.1016/j.ces.2015.11.001.

[40] B. Tohidi, A. Danesh, A.C. Todd, R.W. Burgass, K.K. Østergaard, Equilibrium data and thermodynamic modelling of cyclopentane and neopentane hydrates, Fluid Phase Equilib. 138 (1997) 241–250. doi:10.1016/S0378-3812(97)00164-7.

[41] Q.N. Lv, X. Sen Li, Z.Y. Chen, J.C. Feng, Phase equilibrium and dissociation enthalpies for hydrates of various water-insoluble organic promoters with methane, J. Chem. Eng. Data. 58 (2013) 3249–3253. doi:10.1021/je4007025.

[42] D. Corak, T. Barth, S. Høiland, T. Skodvin, R. Larsen, T. Skjetne, Effect of subcooling and amount of hydrate former on formation of cyclopentane hydrates in brine, Desalination. 278 (2011) 268–274. doi:10.1016/j.desal.2011.05.035.

[43] F. Li, Z. Chen, H. Dong, C. Shi, B. Wang, L. Yang, Z. Ling, Promotion e ff ect of graphite on cyclopentane hydrate based desalination, Desalination. 445 (2018) 197–203. doi:10.1016/j.desal.2018.08.011.

[44] S. Hong, S. Moon, Y. Lee, S. Lee, Y. Park, Investigation of thermodynamic and kinetic effects of cyclopentane derivatives on CO2 hydrates for potential application to seawater

desalination, Chem. Eng. J. 363 (2019) 99–106. doi:10.1016/j.cej.2019.01.108.

[45] Q. Wang, D. Han, Z. Wang, Q. Ma, D. Wang, D. Wang, Lattice Boltzmann modeling for hydrate formation in brine Dalian University of Technology, Chem. Eng. J. (2019). doi:10.1016/j.cej.2019.02.060.

[46] C. McAuliffe, Solubility in Water of Paraffin, Cycloparaffin, Olefin, Acetylene, Cycloolefin, and Aromatic Hydrocarbons1, J. Phys. Chem. 70 (1966) 1267–1275. doi:DOI: 10.1021/j100876a049.

[47] J. nan Zheng, M. jun Yang, Y. Liu, D. yong Wang, Y. chen Song, Effects of cyclopentane on CO2 hydrate formation and dissociation as a co-guest molecule for desalination, J. Chem. Thermodyn. 104 (2017) 9–15. doi:10.1016/j.jct.2016.09.006.

[48] J. Lee, Y.K. Jin, Y. Seo, Characterization of cyclopentane clathrates with gaseous guests for gas storage and separation, Chem. Eng. J. 338 (2018) 572–578. doi:10.1016/J.CEJ.2018.01.054.

[49] W.L. Zhao, D.L. Zhong, C. Yang, Prediction of phase equilibrium conditions for gas hydrates formed in the presence of cyclopentane or cyclohexane, Fluid Phase Equilib. 427 (2016) 82–89. doi:10.1016/j.fluid.2016.06.044.

[50] D. Jianwei, L. Deqing, L. Dongliang, L. Xinjun, Experimental determination of the equilibrium conditions of binary gas hydrates of cyclopentane + oxygen, cyclopentane + nitrogen, and cyclopentane + hydrogen, Ind. Eng. Chem. Res. 49 (2010) 11797–11800. doi:10.1021/ie101339j.

[51] S. Baek, J. Min, J.W. Lee, Inhibition effects of activated carbon particles on gas hydrate formation at oil–water interfaces, RSC Adv. 5 (2015) 58813–58820. doi:10.1039/C5RA08335D.

[52] Y. Matsumoto, T. Makino, T. Sugahara, K. Ohgaki, Phase equilibrium relations for binary mixed hydrate systems composed of carbon dioxide and cyclopentane derivatives, Fluid Phase Equilib. 362 (2014) 379–382. doi:10.1016/j.fluid.2013.10.057.

[53] P.J. Herslund, N. Daraboina, K. Thomsen, J. Abildskov, N. von Solms, Measuring and modelling of the combined thermodynamic promoting effect of tetrahydrofuran and cyclopentane on carbon dioxide hydrates, Fluid Phase Equilib. 381 (2014) 20–27. doi:10.1016/j.fluid.2014.08.015.

[54] J.N. Zheng, M. Yang, B. Chen, Y. Song, D. Wang, Research on the CO_2Gas Uptake of

Different Hydrate Structures with Cyclopentane or Methyl-cyclopentane as Co-guest Molecules, Energy Procedia. 105 (2017) 4133–4139. doi:10.1016/j.egypro.2017.03.877.

[55] Q. Lv, X. Li, Raman Spectroscopic Studies on Microscopic Mechanism of CP - CH_4 Mixture Hydrate, Energy Procedia. 142 (2017) 3264–3269. doi:10.1016/j.egypro.2017.12.501.

[56] A.H. Mohammadi, D. Richon, Phase Equilibria of Clathrate Hydrates of Tetrahydrofuran+Hydrogen Sulfide and Tetrahydroduran+Methane, J. Chem. Eng. Data. 55 (2009) 982–984. doi:10.1021/je9004257.

[57] Palmer, H. A. Characterization of hydrocarbon-type hydrates. Ph.D.Thesis, University of Oklahoma, Norman, OK, 1950.

[58] D.W.Davidson, Clathrate Hydrates, in: F. Franks (Ed.), Water Cryst. Hydrates Aqueous Solut. Simple Nonelectrolytes, 2nd ed., Springer Science+Business Media, New York, 1973.

[59] S.S. Fan, D.Q. Liang, K.H. Guo, Hydrate equilibrium conditions for cyclopentane and a quaternary cyclopentane-rich mixture, J. Chem. Eng. Data. 46 (2001) 930–932. doi:10.1021/je010026l.

[60] M. Nakajima, R. Ohinura, Y.H. Mori, Clathrate hydrate formation from cyclopentane-in-water emulsions, Ind. Eng. Chem. Res. 47 (2008) 8933–8939. doi:10.1021/ie800949k.

[61] C.A. Whitman, R. Mysyk, M.A. White, Investigation of factors affecting crystallization of cyclopentane clathrate hydrate, J. Chem. Phys. 129 (2008). doi:10.1063/1.3005379.

[62] J.W. Nicholas, L.E. Dieker, E.D. Sloan, C.A. Koh, Assessing the feasibility of hydrate deposition on pipeline walls-Adhesion force measurements of clathrate hydrate particles on carbon steel, J. Colloid Interface Sci. 331 (2009) 322–328. doi:10.1016/j.jcis.2008.11.070.

[63] J.S. Zhang, J.W. Lee, Equilibrium of hydrogen + cyclopentane and carbon dioxide + cyclopentane binary hydrates, J. Chem. Eng. Data. 54 (2009) 659–661. doi:10.1021/je800219k.

[64] R. Sakemoto, H. Sakamoto, K. Shiraiwa, R. Ohmura, T. Uchida, Clathrate hydrate crystal growth at the seawater/hydrophobic-guest-liquid interface, Cryst. Growth Des. 10 (2010) 1296–1300. doi:10.1021/cg901334z.

[65] E.G. Dirdal, C. Arulanantham, H. Sefidroodi, M.A. Kelland, Can cyclopentane hydrate

formation be used to rank the performance of kinetic hydrate inhibitors?, Chem. Eng. Sci. 82 (2012) 177–184. doi:10.1016/j.ces.2012.07.043.

[66] H. Sefidroodi, E. Abrahamsen, M.A. Kelland, Investigation into the strength and source of the memory effect for cyclopentane hydrate, Chem. Eng. Sci. 87 (2013) 133–140. doi:10.1016/j.ces.2012.10.018.

[67] R. Ambekar, Equilibrium conditions of Hydrate-forming pickering emulsions (M.S. thesis), City University of New York, New York, NY, 2012.

[68] G. Zylyftari, J.W. Lee, J.F. Morris, Salt effects on thermodynamic and rheological properties of hydrate forming emulsions, Chem. Eng. Sci. 95 (2013) 148–160. doi:10.1016/j.ces.2013.02.056.

[69] S. Han, J.Y. Shin, Y.W. Rhee, S.P. Kang, Enhanced efficiency of salt removal from brine for cyclopentane hydrates by washing, centrifuging, and sweating, Desalination. 354 (2014) 17–22. doi:10.1016/j.desal.2014.09.023.

[70] Hongfei Xu. Hydrate Desalination Using Cyclopentane Hydrates At Atmospheric Pressure. M.S. Thesis, Colorado School of Mines, U.S.A, 2014.

[71] M. Mitarai, M. Kishimoto, D. Suh, R. Ohmura, Surfactant effects on the crystal growth of clathrate hydrate at the interface of water and hydrophobic-guest liquid, Cryst. Growth Des. 15 (2015) 812–821. doi:10.1021/cg501613a.

[72] M.L. Martinez de Baños, O. Carrier, P. Bouriat, D. Broseta, Droplet-based millifluidics as a new tool to investigate hydrate crystallization: Insights into the memory effect, Chem. Eng. Sci. 123 (2015) 564–572. doi:10.1016/j.ces.2014.11.018.

[73] S. Baek, J. Min, J.W. Lee, Equilibria of cyclopentane hydrates with varying HLB numbers of sorbitan monoesters in water-in-oil emulsions, Fluid Phase Equilib. 413 (2016) 41–47. doi:10.1016/j.fluid.2015.10.018.

[74] E.P. Brown, C.A. Koh, Micromechanical measurements of the effect of surfactants on cyclopentane hydrate shell properties., Phys. Chem. Chem. Phys. 18 (2016) 594–600. doi:10.1039/c5cp06071k.

[75] J. Peixinho, V. Ageorges, B. Duchemin, Growth of Clathrate Hydrates from Water Drops in Cyclopentane, Energy & Fuels. (2017) acs.energyfuels.7b02740. doi:10.1021/acs.energyfuels.7b02740.

[76] N. Hobeika, M.L. Martinez De Baños, P. Bouriat, D. Broseta, R. Brown, High-Resolution

Optical Microscopy of Gas Hydrates, in: Gas Hydrates 1, 2017: pp. 113–144. doi:10.1002/9781119332688.ch3.

[77] H. Delroisse, J.-P. Torré, C. Dicharry, Effect of a Hydrophilic Cationic Surfactant on Cyclopentane Hydrate Crystal Growth at the Water/Cyclopentane Interface, Cryst. Growth Des. 17 (2017) 5098–5107. doi:10.1021/acs.cgd.7b00241.

[78] H. Delroisse, F. Plantier, L. Marlin, C. Dicharry, L. Frouté, R. André, J. Torré, Determination of thermophysical properties of cyclopentane hydrate using a stirred calorimetric cell, J. Chem. Thermodyn. 125 (2018) 136–141. doi:10.1016/j.jct.2018.05.023.

[79] A. Masoudi, P. Jafari, M. Nazari, V. Kashyap, B. Eslami, P. Irajizad, P. Jafari, M. Nazari, V. Kashyap, B. Eslami, P. Irajizad, An in situ method on kinetics of gas hydrates An in situ method on kinetics of gas hydrates, Rev. Sci. Instrum. 035111 (2019). doi:10.1063/1.5082333.

[80] Z.M. Aman, E.P. Brown, E.D. Sloan, A.K. Sum, C. a. Koh, Interfacial mechanisms governing cyclopentane clathrate hydrate adhesion/cohesion, Phys. Chem. Chem. Phys. 13 (2011) 19796. doi:10.1039/c1cp21907c.

[81] P.U. Karanjkar, J.W. Lee, J.F. Morris, Surfactant Effects on Hydrate Crystallization at the Water–Oil Interface: Hollow-Conical Crystals, Cryst. Growth Des. 12 (2012) 3817–3824. doi:10.1021/cg300255g.

[82] M. Perez, Gibbs-Thomson effects in phase transformations, Scr. Mater. 52 (2005) 709–712. doi:10.1016/j.scriptamat.2004.12.026.

[83] S.-S. Fan, T.-M. Guo, Hydrate Formation of CO_2-Rich Binary and Quaternary Gas Mixtures in Aqueous Sodium Chloride Solutions, J. Chem. Eng. Data. 44 (1999) 829–832. doi:10.1021/je990011b.

[84] J.P. Mericq, S. Laborie, C. Cabassud, Vacuum membrane distillation of seawater reverse osmosis brines, Water Res. 44 (2010) 5260–5273. doi:10.1016/j.watres.2010.06.052.

[85] T.J. Itsuno, K.H. Amabe, Vacuum Distillation System Aiming to Use Solar-Heat for Desalination, J. Arid L. Stud. 155 (2012) 153–155.

[86] A.T. Trueba, L.J. Rovetto, L.J. Florusse, M.C. Kroon, C.J. Peters, Phase equilibrium measurements of structure II clathrate hydrates of hydrogen with various promoters, Fluid Phase Equilib. 307 (2011) 6–10. doi:10.1016/j.fluid.2011.04.025.

[87] M. Kishimoto, S. Iijima, R. Ohmura, Crystal growth of clathrate hydrate at the interface between seawater and hydrophobic-guest liquid: Effect of elevated salt concentration, Ind. Eng. Chem. Res. 51 (2012) 5224–5229. doi:10.1021/ie202785z.

[88] S. Ho-Van, B. Bouillot, J. Douzet, S. Maghsoodloo Babakhani, J.-M. Herri, Implementing Cyclopentane Hydrates Phase Equilibrium Data and Simulations in Brine Solutions, Ind. Eng. Chem. Res. 57 (2018) 14774 -14783. doi:10.1021/acs.iecr.8b02796.

[89] Sloan D, Koh C, K.Sum A. Natural Gas Hydrate in Flow Assurance. Gulf Professional Pub./Elsevier; 2011.

[90] J.H. Cha, Y. Seol, Increasing gas hydrate formation temperature for desalination of high salinity produced water with secondary guests, ACS Sustain. Chem. Eng. 1 (2013) 1218–1224. doi:10.1021/sc400160u.

[91] Q.N. Lv, X. Sen Li, Z.Y. Chen, Formation of cyclopentane - methane hydrates in brine systems and characteristics of dissolved ions, Appl. Energy. 184 (2016) 482–490. doi:10.1016/j.apenergy.2016.10.035.

[92] Y. Zhang, S.M. Sheng, X.D. Shen, X.B. Zhou, W.Z. Wu, X.P. Wu, D.Q. Liang, Phase Equilibrium of Cyclopentane + Carbon Dioxide Binary Hydrates in Aqueous Sodium Chloride Solutions, J. Chem. Eng. Data. 62 (2017) 2461–2465. doi:10.1021/acs.jced.7b00404.

[93] A.H. Mohammadi, D. Richon, Phase equilibria of clathrate hydrates of methyl cyclopentane, methyl cyclohexane, cyclopentane or cyclohexane+carbon dioxide, Chem. Eng. Sci. 64 (2009) 5319–5322. doi:10.1016/j.ces.2009.09.048.

[94] M. Wang, Z.G. Sun, C.H. Li, A.J. Zhang, J. Li, C.M. Li, H.F. Huang, Equilibrium Hydrate Dissociation Conditions of CO_2+ HCFC141b or Cyclopentane, J. Chem. Eng. Data. 61 (2016) 3250–3253. doi:10.1021/acs.jced.6b00333.

[95] A. Galfré, M. Kwaterski, P. Braîntuas, A. Cameirao, J.M. Herri, Clathrate hydrate equilibrium data for the gas mixture of carbon dioxide and nitrogen in the presence of an emulsion of cyclopentane in water, J. Chem. Eng. Data. 59 (2014) 592–602. doi:10.1021/je4002587.

[96] Z.Y. Chen, Q.P. Li, Z.Y. Yan, K.F. Yan, Z.Y. Zeng, X. Sen Li, Phase equilibrium and dissociation enthalpies for cyclopentane + methane hydrates in NaCl aqueous solutions, J. Chem. Eng. Data. 55 (2010) 4444–4449. doi:10.1021/je100597e.

[97] Q. Lv, Y. Song, X. Li, Kinetic study on the process of cyclopentane + methane hydrate formation in NaCl solution, Energy & Fuels. 30 (2016) 1310–1316. doi:10.1021/acs.energyfuels.5b02634.

[98] Q. Lv, X. Zang, X. Li, G. Li, Effect of seawater ions on cyclopentane-methane hydrate phase equilibrium, Fluid Phase Equilib. 458 (2018) 272–277. doi:10.1016/j.fluid.2017.11.031.

[99] H. Yang, S. Fan, X. Lang, Y. Wang, X. Sun, Hydrate dissociation conditions for mixtures of air + tetrahydrofuran, air + cyclopentane, and air + tetra-n-butyl ammonium bromide, J. Chem. Eng. Data. 57 (2012) 1226–1230. doi:10.1021/je201330j.

[100] S. Takeya, K. Yasuda, R. Ohmura, Phase equilibrium for structure II hydrates formed with methylfluoride coexisting with cyclopentane, fluorocyclopentane, cyclopentene, or tetrahydropyran, J. Chem. Eng. Data. 53 (2008) 531–534. doi:10.1021/je700624q.

[101] S. Takeya, R. Ohmura, Phase Equilibrium for Structure II Hydrates Formed with Krypton Co-existing with Cyclopentane, Cyclopentene, or Tetrahydropyran, J. Chem. Eng. Data. 51 (2006) 1880–1883. doi:10.1021/je060233r.

[102] S. Imai, K. Okutani, R. Ohmura, Y.H. Mori, Phase Equilibrium for Clathrate Hydrates Formed with Difluoromethane + either Cyclopentane or Tetra- n -butylammonium Bromide, J. Chem. Eng. Data. 50 (2005) 1783–1786. doi:10.1021/je050212h.

[103] H. Komatsu, H. Yoshioka, M. Ota, Phase Equilibrium Measurements of Hydrogen− Tetrahydrofuran and Hydrogen− Cyclopentane Binary Clathrate Hydrate Systems, J. Chem. Eng. Data. (2010) 2214–2218. doi:10.1021/je900767h.

[104] P. Di Profio, V. Canale, R. Germani, S. Arca, A. Fontana, Reverse micelles enhance the formation of clathrate hydrates of hydrogen, J. Colloid Interface Sci. 516 (2018) 224–231. doi:10.1016/j.jcis.2018.01.059.

[105] D.L. Zhong, N. Daraboina, P. Englezos, Recovery of CH4 from coal mine model gas mixture (CH_4/N_2) by hydrate crystallization in the presence of cyclopentane, Fuel. 106 (2013) 425–430. doi:10.1016/j.fuel.2013.01.029.

[106] Q. Lv, L. Li, X. Li, Z. Chen, Clathrate hydrate dissociation conditions and structure of the methane + cyclopentane + trimethylene sulfide hydrate in NaCl aqueous solution, Fluid Phase Equilib. 425 (2016) 305–311. doi:10.1016/j.fluid.2016.06.020.

[107] F. Tzirakis, P. Stringari, N. von Solms, C. Coquelet, G. Kontogeorgis, Hydrate

equilibrium data for the CO_2+ N_2 system with the use of tetra-n-butylammonium bromide (TBAB), cyclopentane (CP) and their mixture, Fluid Phase Equilib. 408 (2016) 240–247. doi:10.1016/j.fluid.2015.09.021.

[108] J. Zhang, P. Yedlapalli, J.W. Lee, Thermodynamic analysis of hydrate-based pre-combustion capture of CO_2, Chem. Eng. Sci. 64 (2009) 4732–4736. doi:10.1016/j.ces.2009.04.041.

[109] H. Liu, J. Wang, G. Chen, B. Liu, A. Dandekar, B. Wang, X. Zhang, C. Sun, Q. Ma, High-efficiency separation of a CO_2/H_2 mixture via hydrate formation in W/O emulsions in the presence of cyclopentane and TBAB, Int. J. Hydrogen Energy. 39 (2014) 7910–7918. doi:10.1016/j.ijhydene.2014.03.094.

[110] S. Li, S. Fan, J. Wang, X. Lang, Y. Wang, Clathrate hydrate capture of CO_2 from simulated flue gas with cyclopentane/water emulsion, Chinese J. Chem. Eng. 18 (2010) 202–206. doi:10.1016/S1004-9541(08)60343-2.

[111] D.L. Zhong, K. Ding, C. Yang, Y. Bian, J. Ji, Phase equilibria of clathrate hydrates formed with CH_4 + N_2 + O_2 in the presence of cyclopentane or cyclohexane, J. Chem. Eng. Data. 57 (2012) 3751–3755. doi:10.1021/je301024v.

[112] J.-M. Herri, A. Bouchemoua, M. Kwaterski, A. Fezoua, Y. Ouabbas, A. Cameirao, Gas hydrate equilibria for CO_2–N_2 and CO_2–CH_4 gas mixtures—Experimental studies and thermodynamic modelling, Fluid Phase Equilib. 301 (2011) 171–190. doi:10.1016/j.fluid.2010.09.041.

[113] H. Yang, Z. Xu, M. Fan, R.B. Slimane, A.E. Bland, I. Wright, Progress in carbon dioxide seperation and capture: A review, J. Environ. Sci. 20 (2008) 14–27. doi:10.1016/S1001-0742(08)60002-9.

[114] X. Sen Li, C.G. Xu, Z.Y. Chen, J. Cai, Synergic effect of cyclopentane and tetra-n-butyl ammonium bromide on hydrate-based carbon dioxide separation from fuel gas mixture by measurements of gas uptake and X-ray diffraction patterns, Int. J. Hydrogen Energy. 37 (2012) 720–727. doi:10.1016/j.ijhydene.2011.09.053.

[115] P.J. Herslund, Thermodynamic and Process Modelling of Gas Hydrate Systems in CO_2 Capture Processes, Technical University of Denmark, 2013.

[116] J. Zheng, Z. Bao-yong, Q. Wu, P. Linga, Kinetic evaluation of cyclopentane as a promoter for CO_2 capture via clathrate process employing different contact modes, Sustain. Chem.

Eng. (2018). doi:10.1021/acssuschemeng.8b02187.

[117] M. Yang, J. Zheng, W. Liu, Y. Liu, Y. Song, Effects of C3H8 on hydrate formation and dissociation for integrated CO_2 capture and desalination technology, Energy. 93 (2015) 1971–1979. doi:10.1016/j.energy.2015.10.076.

[118] M. Sarshar, a H. Sharafi, Simultaneous water desalination and CO_2 capturing by hydrate formation, Desalin. Water Treat. 28 (2011) 59–64. doi:10.5004/dwt.2011.2201.

[119] Y.-N. Lv, S.-S. Wang, C.-Y. Sun, J. Gong, G.-J. Chen, Desalination by forming hydrate from brine in cyclopentane dispersion system, Desalination. 413 (2017) 217–222. doi:10.1016/j.desal.2017.03.025.

[120] L.C. Ho, P. Babu, R. Kumar, P. Linga, HBGS (hydrate based gas separation) process for carbon dioxide capture employing an unstirred reactor with cyclopentane, Energy. 63 (2013) 252–259. doi:10.1016/j.energy.2013.10.031.

[121] M.L. Martinez de Baños, Mechanisms of formation and dissociation of cyclopentane hydrates, Ph.D.Thesis, Université de Pau et des Pays de l'Adour, 2015.

[122] M. Li, J. Tian, C. Liu, K. Geng, Effects of sorbitan monooleate on the interactions between cyclopentane hydrate particles and water droplets, J. Dispers. Sci. Technol. 39 (2018) 360–366. doi:10.1080/01932691.2017.1318706.

[123] S. Ho-van, B. Bouillot, D. Garcia, J. Douzet, A. Cameirao, S. Maghsoodloo-, Crystallization mechanisms and rates of Cyclopentane Hydrates formation in Brine, Chem. Eng. Technol. (2019) 1–21. doi:10.1002/ceat.201800746.

[124] H. Xu, M.N. Khan, C.J. Peters, E.D. Sloan, A.K. Sum, C.A. Koh, Hydrate Desalination Using Cyclopentane Hydrates At Atmospheric Pressure, in: Proc. 8th Int. Conf. Gas Hydrates, Beijing, China, 2014: pp. 1–7.

[125] L. Cai, B.A. Pethica, P.G. Debenedetti, S. Sundaresan, Formation kinetics of cyclopentane-methane binary clathrate hydrate, Chem. Eng. Sci. 119 (2014) 147–157. doi:10.1016/j.ces.2014.08.025.

[126] Y.A. Lim, P. Babu, R. Kumar, P. Linga, Morphology of carbon dioxide-hydrogen-cyclopentane hydrates with or without sodium dodecyl sulfate, Cryst. Growth Des. 13 (2013) 2047–2059. doi:10.1021/cg400118p.

[127] Q. Lv, L. Li, X. Li, Z. Chen, Formation Kinetics of Cyclopentane + Methane Hydrates in Brine Water Systems and Raman Spectroscopic Analysis, Energy and Fuels. 29 (2015)

6104–6110. doi:10.1021/acs.energyfuels.5b01416.

[128] C.J. Brown, X. Ni, Evaluation of rate of cyclopentane hydrate formation in an oscillatory baffled column using laser induced fluorescence and energy balance, Chem. Eng. J. 157 (2010) 131–139. doi:10.1016/j.cej.2009.11.019.

[129] G. Zylyftari, A. Ahuja, J.F. Morris, Nucleation of cyclopentane hydrate by ice studied by morphology and rheology, Chem. Eng. Sci. 116 (2014) 497–507. doi:10.1016/j.ces.2014.05.019.

[130] P.U. Karanjkar, J.W. Lee, J.F. Morris, Calorimetric investigation of cyclopentane hydrate formation in an emulsion, Chem. Eng. Sci. 68 (2012) 481–491. doi:10.1016/j.ces.2011.10.014.

[131] K. Dann, L. Rosenfeld, J. Accepted, Surfactant effect on hydrate crystallization at oil-water interface, Langmuir. (2018). doi:10.1021/acs.langmuir.8b00333.

[132] C. Lo, J.S. Zhang, a. Couzis, P. Somasundaran, J.W. Lee, Adsorption of Cationic and Anionic Surfactants on Cyclopentane Hydrates, J. Phys. Chem. C. 114 (2010) 13385–13389. doi:10.1021/jp102846d.

[133] C. Lo, J.S. Zhang, P. Somasundaran, S. Lu, a. Couzis, J.W. Lee, Adsorption of Surfactants on Two Different Hydrates, Langmuir. 24 (2008) 12724–12726. doi:10.1021/la802362m.

[134] A. Erfani, F. Varaminian, Kinetic promotion of non-ionic surfactants on cyclopentane hydrate formation, J. Mol. Liq. 221 (2016) 963–971. doi:10.1016/j.molliq.2016.06.058.

[135] Li, Huijuan, Du, Jianwei and Wang, Liguang (2013). Effect of surfactant-coated particles on clathrate hydrate formation. In: Chemeca 2013: Challenging Tomorrow. Chemeca 2013: Australasian Conference on Chemical Engineering, Brisbane, QLD, Australia, (1-5). 29 September-2 October, 2013.

[136] C. Lo, J. Zhang, P. Somasundaran, J.W. Lee, Raman spectroscopic studies of surfactant effect on the water structure around hydrate guest molecules, J. Phys. Chem. Lett. 1 (2010) 2676–2679. doi:10.1021/jz1009967.

[137] R.Z.J. Wu, Experimental studies of gas hydrate formation, Ph.D.Thesis, The University of Western Australia, 2014.

[138] N. Abojaladi, M.A. Kelland, Can cyclopentane hydrate formation be used to screen the performance of surfactants as LDHI anti-agglomerants at atmospheric pressure?, Chem.

Eng. Sci. 152 (2016) 746–753. doi:10.1016/j.ces.2016.06.067.

[139] X. Li, L. Negadi, A. Firoozabadi, Anti-agglomeration in cyclopentane hydrates from bio- and co-surfactants, Energy and Fuels. 24 (2010) 4937–4943. doi:10.1021/ef100622p.

[140] J.S. Zhang, C. Lo, A. Couzis, P. Somasundaran, J. Wu, J.W. Lee, Adsorption of kinetic inhibitors on clathrate hydrates, J. Phys. Chem. C. 113 (2009) 17418–17420. doi:10.1021/jp907796d.

[141] S.A. Morrissy, A.J. McKenzie, B.F. Graham, M.L. Johns, E.F. May, Z.M. Aman, Reduction of Clathrate Hydrate Film Growth Rate by Naturally Occurring Surface Active Components, Energy & Fuels. 31 (2017) 5798–5805. doi:10.1021/acs.energyfuels.6b02942.

[142] R. Ohmura, M. Ogawa, K. Yasuoka, Y.H. Mori, Statistical Study of Clathrate-Hydrate Nucleation in a Water/Hydrochlorofluorocarbon System: Search for the Nature of the "Memory Effect," J. Phys. Chem. B. 107 (2003) 5289–5293. doi:10.1021/jp027094e.

[143] P. Englezos, Clathrate Hydrates., Ind. Eng. Chem. Res. 32 (1993) 1251–1274. doi:10.1021/ie00019a001.

[144] D. Kashchiev, A. Firoozabadi, Induction time in crystallization of gas hydrates, J. Cryst. Growth. 250 (2003) 499–515. doi:10.1016/S0022-0248(02)02461-2.

[145] L.C. Jacobson, W. Hujo, V. Molinero, Nucleation pathways of clathrate hydrates: Effect of guest size and solubility, J. Phys. Chem. B. 114 (2010) 13796–13807. doi:10.1021/jp107269q.

[146] T. Uchida, I.Y. Ikeda, S. Takeya, T. Ebinuma, J. Nagao, H. Narita, CO_2 hydrate film formation at the boundary between CO_2 and water: Effects of temperature, pressure and additives on the formation rate, J. Cryst. Growth. 237–239 (2002) 383–387. doi:10.1016/S0022-0248(01)01822-X.

[147] K. Saito, A.K. Sum, R. Ohmura, Correlation of Hydrate-Film Growth Rate at the Guest / Liquid-Water Interface to Mass Transfer Resistance, Society. 7 (2010) 7102–7103. doi:Doi 10.3390/En5010092.

[148] K. Saito, M. Kishimoto, R. Tanaka, R. Ohmura, Crystal growth of clathrate hydrate at the interface between hydrocarbon gas mixture and liquid water, Cryst. Growth Des. 11 (2011) 295–301. doi:10.1021/cg101310z.

[149] E.M. Freer, M.S. Selim, E.D.S. Jr, Methane hydrate film growth kinetics, Fluid Phase

Equilib. 185 (2001) 65–75. doi: 10.1016/S0378-3812(01)00457-5.

[150] B.Z. Peng, A. Dandekar, C.Y. Sun, H. Luo, Q.L. Ma, W.X. Pang, G.J. Chen, Hydrate film growth on the surface of a gas bubble suspended in water, J. Phys. Chem. B. 111 (2007) 12485–12493. doi:10.1021/jp074606m.

[151] C.J. Taylor, K.T. Miller, C.A. Koh, E.D. Sloan, Macroscopic investigation of hydrate film growth at the hydrocarbon/water interface, Chem. Eng. Sci. 62 (2007) 6524–6533. doi:10.1016/j.ces.2007.07.038.

[152] M. Karamoddin, F. Varaminian, Water purification by freezing and gas hydrate processes, and removal of dissolved minerals (Na^+, K^+, Mg^{2+}, Ca^{2+}), J. Mol. Liq. 223 (2016) 1021–1031. doi:10.1016/j.molliq.2016.08.099.

[153] S.R. Davies, J.W. Lachance, E.D. Sloan, C.A. Koh, High-Pressure Differential Scanning Calorimetry Measurements of the Mass Subcooling, Industrial & Engineering Chemistry Research. 49 (2010) 12319–12326. doi: 10.1021/ie1017173

[154] S. Takeya, A. Hori, T. Hondoh, T. Uchida, Freezing-memory effect of water on nucleation of CO_2 hydrate crystals, J. Phys. Chem. B. 104 (2000) 4164–4168. doi:10.1021/jp993759+.

[155] J.S. PARENT, P. BISHNOI, Investigations Into the Nucleation Behaviour of Methane Gas Hydrates, Chem. Eng. Commun. 144 (1996) 51–64. doi:10.1080/00986449608936444.

[156] C. Duchateau, C. Dicharry, J.-L. Peytavy, P. Glénat, T.-E. Pou, M. Hidalgo, Laboratory Evaluation of Kinetic Hydrate Inhibitors : a New Procedure for Improving the Reproducibility of Measurements, Icgh2008. 23 (2008) 962–966.

[157] C. Duchateau, P. Glénat, T.E. Pou, M. Hidalgo, C. Dicharry, Hydrate precursor test method for the laboratory evaluation of kinetic hydrate inhibitors, Energy and Fuels. 24 (2010) 616–623. doi:10.1021/ef900797e.

[158] L. Jensen, K. Thomsen, N. Von Solms, Inhibition of structure I and II gas hydrates using synthetic and biological kinetic inhibitors, Energy and Fuels. 25 (2011) 17–23. doi:10.1021/ef100833n.

[159] M. a Kelland, History of the Development of Low Dosage Hydrate Inhibitors, Energy Fuels. 20 (2006) 825–847. doi:10.1021/ef050427x.

[160] Y. Xie, K. Guo, D. Liang, S. Fan, J. Gu, J. Chen, Gas hydrate fast nucleation from melting ice and quiescent growth along vertical heat transfer tube, Sci. China Ser. B Chem. 48

(2005) 75–82. doi:10.1007/BF02990916.

[161] E.D. Sloan, F. Fleyfel, A Molecular Mechanism for Gas Hydrate Nucleation from Ice, AIChE J. 37 (1991) 1281–1292. doi:10.1002/aic.690370902

[162] M. Rahmati-abkenar, M. Manteghian, H. Pahlavanzadeh, Nucleation of ethane hydrate in water containing silver nanoparticles, Mater. Des. 126 (2017) 190–196. doi:10.1016/j.matdes.2017.04.051.

[163] S. Abedi-farizhendi, M. Rahmati-abkenar, M. Manteghian, J.S. Yekshaveh, V. Zahmatkeshan, Kinetic study of propane hydrate in the presence of carbon nanostructures and SDS, J. Pet. Sci. Eng. 172 (2019) 636–642. doi:10.1016/j.petrol.2018.04.075.

[164] O. Nashed, B. Partoon, B. Lal, K.M. Sabil, A. Mohd, Review the impact of nanoparticles on the thermodynamics and kinetics of gas hydrate formation, 55 (2018) 452–465. doi:10.1016/j.jngse.2018.05.022.

[165] S. Said, V. Govindaraj, J. Herri, Y. Ouabbas, A study on the influence of nanofluids on gas hydrate formation kinetics and their potential: Applicatin to the CO_2 capture process, J. Nat. Gas Sci. Eng. 32 (2016) 95–108. doi:10.1016/j.jngse.2016.04.003.

[166] C.Y. Lo, The role of surface active agents on hydrate formation. Ph.D.Thesis, The City University of New York, 2011.

[167] A.N. Nesterov, A.M. Reshetnikov, A.Y. Manakov, T. V. Rodionova, E.A. Paukshtis, I.P. Asanov, S.P. Bardakhanov, A.I. Bulavchenko, Promotion and inhibition of gas hydrate formation by oxide powders, J. Mol. Liq. 204 (2015) 118–125. doi:10.1016/j.molliq.2015.01.037.

[168] B. Zarenezhad, Accurate prediction of the interfacial tension of surfactant/fluid mixtures during gas hydrate nucleation: The case of SDS surfactant-based systems near ethylene hydrate formation region, J. Mol. Liq. 191 (2014) 161–165. doi:10.1016/j.molliq.2013.12.005.

[169] Z.M. Aman, K. Olcott, K. Pfeiffer, E.D. Sloan, A.K. Sum, C.A. Koh, Surfactant adsorption and interfacial tension investigations on cyclopentane hydrate, Langmuir. 29 (2013) 2676–2682. doi:10.1021/la3048714.

[170] Z.M. Aman, C.A. Koh, Interfacial phenomena in gas hydrate systems, Chem. Soc. Rev. 45 (2016) 1678–1690. doi:10.1039/C5CS00791G.

[171] BMH Abdulkader, Cyclopentane Hydrate for Hydrate Wetting Studies, M.S. Thesis,

University of Bergen, 2013.

[172] A. Ahuja, G. Zylyftari, J.F. Morris, Yield stress measurements of cyclopentane hydrate slurry, J. Nonnewton. Fluid Mech. 220 (2015) 116–125. doi:10.1016/j.jnnfm.2014.11.007.

[173] G. Zylyftari, A. Ahuja, J.F. Morris, Modeling Oilfield Emulsions: Comparison of Cyclopentane Hydrate and Ice, Energy and Fuels. 29 (2015) 6286–6295. doi:10.1021/acs.energyfuels.5b01431.

[174] H. Delroisse, G. Barreto, J. Torré, C. Dicharry, Evaluation of the Performance of a New Biodegradable AA-LDHI in Cyclopentane Hydrate and CH_4/C_3H_8 Gas Hydrate Systems, in: SPE Middle East Oil Gas Show Conf., Manama, 2019: pp. 1–13. doi:10.2118/195054-MS.

[175] G. Aspenes, L.E. Dieker, Z.M. Aman, S. Høiland, A.K. Sum, C.A. Koh, E.D. Sloan, Adhesion force between cyclopentane hydrates and solid surface materials, J. Colloid Interface Sci. 343 (2010) 529–536. doi:10.1016/j.jcis.2009.11.071.

[176] Z.M. Aman, L.E. Dieker, G. Aspenes, A.K. Sum, E.D. Sloan, C.A. Koh, Influence of model oil with surfactants and amphiphilic polymers on cyclopentane hydrate adhesion forces, Energy and Fuels. 24 (2010) 5441–5445. doi:10.1021/ef100762r.

[177] Z. Aman, J.L. William, G. Grasso, E.D. Sloan, A.K. Sum, C.A. Koh, Adhesion Force between Cyclopentane Hydrate and Mineral Surfaces, Langmuir. 29 (2013) 15551–15557. doi:dx.doi.org/10.1021/la403489q.

[178] L.E. Dieker, C.J. Taylor, C.A. Koh, D. Sloan, Micromechanical adhesion force measurements between cyclopentane hydrate particles, Conf. Gas Hydrates. (2011) 2011. doi:http://dx.doi.org/10.1016/j.jcis.2006.10.078.

[179] Zachary M. Aman, Luis E. Zerpa, Giovanny Grasso, William E. Leith, E. Dendy Sloan, Amadeu K. Sum, and Carolyn A. Koh, Interfacial Tension and Mineral Adhesion Properties of Cyclopentane Hydrate. Unconventional Resources Technology Conference, Denver, Colorado, 12-14 August 2013: pp. 2265-2268. doi:10.1190/urtec2013-235.

[180] A. Das, T.A. Farnham, S. Bengaluru Subramanyam, K.K. Varanasi, Designing Ultra-Low Hydrate Adhesion Surfaces by Interfacial Spreading of Water-Immiscible Barrier Films, ACS Appl. Mater. Interfaces. 9 (2017) 21496–21502. doi:10.1021/acsami.7b00223.

[181] Z.M. Aman, S.E. Joshi, E.D. Sloan, A.K. Sum, C.A. Koh, Micromechanical cohesion force measurements to determine cyclopentane hydrate interfacial properties, J. Colloid

Interface Sci. 376 (2012) 283–288. doi:10.1016/j.jcis.2012.03.019.

[182] E. Brown, M.N. Khan, D. Salmin, J. Wells, S. Wang, C.J. Peters, C.A. Koh, Cyclopentane hydrate cohesion measurements and phase equilibrium predictions, J. Nat. Gas Sci. Eng. 35 (2016) 1435–1440. doi:10.1016/j.jngse.2016.05.016.

[183] P.U. Karanjkar, A. Ahuja, G. Zylyftari, J.W. Lee, J. F. Morris, Rheology of cyclopentane hydrate slurry in a model oil-continuous emulsion, Rheol. Acta. 55 (2016) 235–243. doi:10.1007/s00397-016-0911-1.

[184] B.C. Leopercio, Kinetics of cyclopentane hydrate formation - an interfacial rheology study, M.S. Thesis, Pontifical Catholic University of Rio de Janeiro, PUC-Rio, Brazil. 2016.

[185] A. Ahuja, G. Zylyftari, J.F. Morris, Calorimetric and rheological studies on cyclopentane hydrate-forming water-in-kerosene emulsions, J. Chem. Eng. Data. 60 (2015) 362–368. doi:10.1021/je500609q.

[186] T. He, Z.R. Chong, P. Babu, P. Linga, Techno-economic Evaluation of Cyclopentane Hydrate-Based Desalination with LNG Cold Energy Utilization, Energy Technol. (2019). doi:10.1002/ente.201900212.

[187] Y. Zhang, P.G. Debenedetti, R.K. Prud, B.A. Pethica, Differential Scanning Calorimetry Studies of Clathrate Hydrate Formation, Water. 108 (2004) 16717–16722. doi:10.1021/jp047421d.

[188] L. CAI, Desalination via formation of binary clathrate hydrates, Ph.D.Thesis 2013. Princeton University. USA.

[189] A.C. Archer, A.M. Mendes, R.A. Boaventura, Separation of an Anionic Surfactant by Nanofiltration, Environ. Sci. Technol. 33 (1999) 2758–2764. doi: 10.1021/es980737c.

[190] M. Zahoor, Separation of surfactants from water by granular activated carbon/ultrafiltration hybrid process, Desalin. Water Treat. 3994 (2016). doi:10.1080/19443994.2014.979242.

[191] P. Taylor, J. Kaleta, M. Elektorowicz, The removal of anionic surfactants from water in coagulation process, Env. Technol. (2012) 37–41. doi:10.1080/09593330.2012.733415.

[192] E. Onder, An alternative method for the removal of surfactants from water : Electrochemical coagulation, Sep. Purif. Technol. 52 (2007) 527–532. doi:10.1016/j.seppur.2006.06.006.

[193] J. Sima, M. Havelka, V. Holcova, Removal of Anionic Surfactants from Wastewater Using a Constructed Wetland, Chem. Biodivers. 6 (2009) 1350–1363. doi:10.1002/cbdv.200900108.

[194] A. Arora, S.S. Cameotra, R. Kumar, C. Balomajumder, Biosurfactant as a Promoter of Methane Hydrate Formation : Thermodynamic and Kinetic Studies, Sci. Rep. (2016) 1–13. doi:10.1038/srep20893.

[195] R.E. Rogers, C. Kothapalli, M.S. Lee, J.R. Woolsey, Catalysis of Gas Hydrates by Biosurfactants in Seawater-Saturated Sand/Clay, Can. J. Chem. Eng. 81 (2003) 973–980. doi:10.1002/cjce.5450810508.

[196] S. Han, Y.W. Rhee, S.P. Kang, Investigation of salt removal using cyclopentane hydrate formation and washing treatment for seawater desalination, Desalination. 404 (2017) 132–137. doi:10.1016/j.desal.2016.11.016.

[197] H. Xu, M.N. Khan, C.J. Peters, E.D. Sloan, C.A. Koh, Hydrate-Based Desalination Using Cyclopentane Hydrates at Atmospheric Pressure, J. Chem. Eng. Data. (2018) acs.jced.7b00815. doi:10.1021/acs.jced.7b00815.

[198] B. Mottet, Method for treating an aqueous solution containing dissolved materials by crystallization of clathrates hydrates, US20170044024A1, 2017.

[199] A.G. Ogienko, A.Y. Manakov, A. V Kurnosov, E. V Grachev, E.G. Larionov, Direct measurement of stoichiometry of the structure H argon gas hydrate synthesized at high pressure, J. Struct. Chem. 46 (2005) 65–69. doi:10.1007/s10947-006-0153-7.

[200] A. Al-Karaghouli, L.L. Kazmerski, Energy consumption and water production cost of conventional and renewable-energy-powered desalination processes, Renew. Sustain. Energy Rev. 24 (2013) 343–356. doi:10.1016/j.rser.2012.12.064.

[201] M. Mahdavi, A.H. Mahvi, S. Nasseri, M. Yunesian, Application of Freezing to the Desalination of Saline Water, Arab. J. Sci. Eng. 36 (2011) 1171–1177. doi:10.1007/s13369-011-0115-z.

[202] M. Ameri, S.S. Mohammadi, M. Hosseini, M. Seifi, Effect of design parameters on multi-effect desalinationsystem specifications, Desalination. 245 (2009) 266–283. doi:10.1016/j.desal.2008.07.012.

[203] J. Imbrogno, J.J. Keating, J. Kilduff, G. Belfort, Critical aspects of RO desalination: A combination strategy, Desalination. 401 (2017) 68–87. doi:10.1016/j.desal.2016.06.033.

[204] K.C. Ng, K. Thu, Y. Kim, A. Chakraborty, G. Amy, Adsorption desalination: An emerging low-cost thermal desalination method, Desalination. 308 (2013) 161–179. doi:10.1016/j.desal.2012.07.030.

[205] M. Elimelech, W.A. Phillip, The Future of Seawater and the Environment: Energy, Technology, and the Environment, Science (80-.). 333 (2011) 712–718. doi:10.1126/science.1200488.

[206] M. Park, N. Park, H. Park, B. Kim, An economic analysis of desalination for potential applicaiton in Korea, Desalination. 114 (1997) 209–221. doi:10.1016/S0011-9164(98)00013-7

[207] K. THU, Adorption desalination: Theory & Experiments, Ph.D.Thesis, National University of Singapore, 2010.

[208] S.A. Kalogirou, Seawater desalination using renewable energy sources, Prog. Energy Combust. Sci. 31 (2005) 242–281. doi:10.1016/j.pecs.2005.03.001.

[209] M.A. Shannon, P.W. Bohn, M. Elimelech, J.G. Georgiadis, B.J. Marĩas, A.M. Mayes, Science and technology for water purification in the coming decades, Nature. 452 (2008) 301–310. doi:10.1038/nature06599.

[210] P.G. Youssef, R.K. Al-Dadah, S.M. Mahmoud, Comparative analysis of desalination technologies, Energy Procedia. 61 (2014) 2604–2607. doi:10.1016/j.egypro.2014.12.258.

[211] J. Javanmardi, M. Moshfeghian, Energy consumption and economic evaluation of water desalination by hydrate phenomenon, Appl. Therm. Eng. 23 (2003) 845–857. doi:10.1016/S1359-4311(03)00023-1.

[212] M. Sangwai, J. S., Patel, R. S., Mekala, P., Mech, D., & Busch, Desalination of Seawater Using Gas Hydrate Technology–Current Status and Future Direction, 18th Conf. Hydraul. Water Resiources, Coast. Environ. Eng. (2013) 434–440.

[213] H. Fakharian, H. Ganji, A. Naderifar, Saline Produced Water Treatment Using Gas Hydrates, J. Environ. Chem. Eng. (2017). doi:10.1016/j.jece.2017.08.008.

[214] P.S. Goh, T. Matsuura, A.F. Ismail, N. Hilal, Recent trends in membranes and membrane processes for desalination, Desalination. 391 (2016) 43–60. doi:10.1016/j.desal.2015.12.016.

[215] Edition, F. (2008). Guidelines for drinking-water quality. WHO Chronicle, 1(3), 334–415.

[216] H.T. El-Dessouky, H.M. Ettouney, Fundamentals of salt water desalination, Elsevier,

2002.

[217] I.C. Karagiannis, P.G. Soldatos, Water desalination cost literature : review and assessment, Desalination. 223 (2008) 448–456. doi:10.1016/j.desal.2007.02.071.

[218] C.S. Bandi, R. Uppaluri, A. Kumar, Global optimization of MSF seawater desalination processes, Desalination. 394 (2016) 30–43. doi:10.1016/j.desal.2016.04.012.

[219] P.M. Williams, M. Ahmad, B.S. Connolly, D.L. Oatley-Radcliffe, Technology for freeze concentration in the desalination industry, Desalination. 356 (2015) 314–327. doi:10.1016/j.desal.2014.10.023.

[220] M.S. Rahman, M. Ahmed, X.D. Chen, Freezing-melting process and desalination: I. review of the state-of-the-art, Sep. Purif. Rev. 35 (2006) 59–96. doi:10.1080/15422110600671734.

[221] A. Alkaisi, R. Mossad, A. Sharifian-Barforoush, A Review of the Water Desalination Systems Integrated with Renewable Energy, Energy Procedia. 110 (2017) 268–274. doi:10.1016/j.egypro.2017.03.138.

[222] J. Hu, Y. Chen, L. Guo, X. Chen, Chemical-free ion exchange and its application for desalination, Desalination. 365 (2015) 144–150. doi:10.1016/j.desal.2015.02.033.

[223] Z.R. Chong, T. He, P. Babu, J. Zheng, P. Linga, Economic evaluation of energy e ffi cient hydrate based desalination utilizing cold energy from lique fi ed natural gas (LNG), Desalination. 463 (2019) 69–80. doi:10.1016/j.desal.2019.04.015.

[224] B.B. Buchanan, Removing salt from sea water, US3027320A, 1962.

[225] M. Karamoddin, F. Varaminian, Water desalination using R141b gas hydrate formation, Desalin. Water Treat. 52 (2014) 2450–2456. doi:10.1080/19443994.2013.798840.

[226] B.O. Bolaji, Z. Huan, Ozone depletion and global warming: Case for the use of natural refrigerant - A review, Renew. Sustain. Energy Rev. 18 (2013) 49–54. doi:10.1016/j.rser.2012.10.008.

[227] T. He, Z. Rong, J. Zheng, Y. Ju, P. Linga, LNG cold energy utilization : Prospects and challenges, Energy. 170 (2019) 557–568. doi:10.1016/j.energy.2018.12.170.

[228] A. Nambiar, P. Babu, Improved Kinetics and Water Recovery with Propane as Co-Guest Gas on the Hydrate-Based Desalination (HyDesal) Process, Chemengineering. (2019). doi:10.3390/chemengineering3010031.

[229] P. Babu, A. Nambiar, T. He, A Review of Clathrate Hydrate Based Desalination to

Strengthen Energy-Water Nexus, ACS Sustain. Chem. Eng. (2018). doi:10.1021/acssuschemeng.8b01616.

[230] G.K. Anderson, Enthalpy of dissociation and hydration number of carbon dioxide hydrate from the Clapeyron equation, J. Chem. Thermodyn. 35 (2003) 1171–1183. doi:10.1016/S0021-9614(03)00093-4.

[231] Q. Nasir, K.K. Lau, B. Lal, Enthalpies of Dissociation of Pure Methane and Carbon Dioxide Gas Hydrate, Int. J. Chem. Nucl. Metall. Mater. Eng. 8 (2014) 785–788.

[232] C.F.S. Lirio, F.L.P. Pessoa, Enthalpy of dissociation of simple and mixed carbon dioxide clathrate hydrate, Chem. Eng. Trans. 32 (2013) 577–582. doi:10.3303/CET1332097.

[233] Compositions, enthalpies of dissociation, and heat capacities in the range 85 to 270 K for clathrate hydrates of methane, ethane, and propane, and enthalpy of dissociation of isobutane hydrate, as determined by a heat-flow calorimeter, J. Chem. Thermodyn. 18 (1986) 915–921. doi:10.1016/0021-9614(86)90149-7.

[234] Y. Bi, T. Guo, T. Zhu, S. Fan, D. Liang, L. Zhang, Influence of volumetric-flow rate in the crystallizer on the gas-hydrate cool-storage process in a new gas-hydrate cool-storage system, Appl. Energy. 78 (2004) 111–121. doi:10.1016/j.apenergy.2003.08.003.